eicosapentaenoic acid on cardiovascular events in statin-treated patients with coronary artery disease. Circ J 2009;73:1283–1290
23. Satoh N, Shimatsu A, Kato Y, et al. Evaluation of the cardio-ankle vascular index, a new indicator of arterial stiffness independent of blood pressure, in obesity and metabolic syndrome. Hypertens Res 2008;31:1921–1930
24. Expert Panel on Detection, Evaluation, and Treatment of High Blood Cholesterol in Adults. Expert Panel on detection, Evaluation, and Treatment of High Blood Cholesterol in Adults. Executive summary of the third report of the National Cholesterol Education Program (NCEP) Expert panel on detection, evaluation, and treatment of high blood cholesterol in adults (Adult Treatment Panel III). JAMA 2001;285:2486–2497
25. Saito Y, Yokoyama M, Origasa H, et al.; JELIS Investigators, Japan. Effects of EPA on coronary artery disease in hypercholesterolemic patients with multiple risk factors: sub-analysis of primary prevention cases from the Japan EPA Lipid Intervention Study (JELIS). Atherosclerosis 2008;200:135–140
26. International clinical harmonization of hemoglobin A1c in Japan: From JDS to NGSP values. The report from "The Committee on the Standardization of Diabetes Mellitus-Related Laboratory Testing" of Japan Diabetes Society (JDS) [article online], 2012. Available from http://www.jds.or.jp/jds_or_jp0/uploads/photos/813.pdf. Accessed 4 February 2012
27. Manigrasso MR, Ferroni P, Santilli F, et al. Association between circulating adiponectin and interleukin-10 levels in android obesity: effects of weight loss. J Clin Endocrinol Metab 2005;90:5876–5879
28. Esposito K, Pontillo A, Giugliano F, et al. Association of low interleukin-10 levels with the metabolic syndrome in obese women. J Clin Endocrinol Metab 2003;88:1055–1058
29. Oh DY, Talukdar S, Bae EJ, et al. GPR120 is an omega-3 fatty acid receptor mediating potent anti-inflammatory and insulin-sensitizing effects. Cell 2010;142:687–698
30. Villalta SA, Rinaldi C, Deng B, Liu G, Fedor B, Tidball JG. Interleukin-10 reduces the pathology of mdx muscular dystrophy by deactivating M1 macrophages and modulating macrophage phenotype. Hum Mol Genet 2011;20:790–805
31. Pinderski Oslund LJ, Hedrick CC, Olvera T, et al. Interleukin-10 blocks atherosclerotic events in vitro and in vivo. Arterioscler Thromb Vasc Biol 1999;19:2847–2853
32. Namiki M, Kawashima S, Yamashita T, et al. Intramuscular gene transfer of interleukin-10 cDNA reduces atherosclerosis in apolipoprotein E-knockout mice. Atherosclerosis 2004;172:21–29
33. Han X, Kitamoto S, Wang H, Boisvert WA. Interleukin-10 overexpression in macrophages suppresses atherosclerosis in hyperlipidemic mice. FASEB J 2010;24:2869–2880
34. Kawashima A, Harada T, Imada K, Yano T, Mizuguchi K. Eicosapentaenoic acid inhibits interleukin-6 production in interleukin-1beta-stimulated C6 glioma cells through peroxisome proliferator-activated receptor-gamma. Prostaglandins Leukot Essent Fatty Acids 2008;79:59–65
35. Thompson PW, Bayliffe AI, Warren AP, Lamb JR. Interleukin-10 is upregulated by nanomolar rosiglitazone treatment of mature dendritic cells and human CD4+ T cells. Cytokine 2007;39:184–191
36. Matsumoto M, Sata M, Fukuda D, et al. Orally administered eicosapentaenoic acid reduces and stabilizes atherosclerotic lesions in ApoE-deficient mice. Atherosclerosis 2008;197:524–533
37. Tishinsky JM, Ma DW, Robinson LE. Eicosapentaenoic acid and rosiglitazone increase adiponectin in an additive and PPARγ-dependent manner in human adipocytes. Obesity (Silver Spring) 2011;19:262–268
38. Kumada M, Kihara S, Ouchi N, et al. Adiponectin specifically increased tissue inhibitor of metalloproteinase-1 through interleukin-10 expression in human macrophages. Circulation 2004;109:2046–2049
39. Ohashi K, Parker JL, Ouchi N, et al. Adiponectin promotes macrophage polarization toward an anti-inflammatory phenotype. J Biol Chem 2010;285:6153–6160
40. Lee SH, Shin MJ, Kim JS, et al. Blood eicosapentaenoic acid and docosahexaenoic acid as predictors of all-cause mortality in patients with acute myocardial infarction—data from Infarction Prognosis Study (IPS) Registry. Circ J 2009;73:2250–2257

ORIGINAL ARTICLE

The Radioprotective 105/MD-1 Complex Contributes to Diet-Induced Obesity and Adipose Tissue Inflammation

Yasuharu Watanabe,[1] Tomoya Nakamura,[1] Sho Ishikawa,[1] Shiho Fujisaka,[2] Isao Usui,[2] Koichi Tsuneyama,[3] Yoshinori Ichihara,[4] Tsutomu Wada,[4] Yoichiro Hirata,[5] Takayoshi Suganami,[6] Hirofumi Izaki,[7] Shizuo Akira,[8] Kensuke Miyake,[9] Hiro-omi Kanayama,[7] Michio Shimabukuro,[10] Masataka Sata,[5] Toshiyasu Sasaoka,[4] Yoshihiro Ogawa,[6] Kazuyuki Tobe,[2] Kiyoshi Takatsu,[1,11] and Yoshinori Nagai[1]

Recent accumulating evidence suggests that innate immunity is associated with obesity-induced chronic inflammation and metabolic disorders. Here, we show that a Toll-like receptor (TLR) protein, radioprotective 105 (RP105)/myeloid differentiation protein (MD)-1 complex, contributes to high-fat diet (HFD)-induced obesity, adipose tissue inflammation, and insulin resistance. An HFD dramatically increased RP105 mRNA and protein expression in stromal vascular fraction of epididymal white adipose tissue (eWAT) in wild-type (WT) mice. RP105 mRNA expression also was significantly increased in the visceral adipose tissue of obese human subjects relative to nonobese subjects. The RP105/MD-1 complex was expressed by most adipose tissue macrophages (ATMs). An HFD increased RP105/MD-1 expression on the M1 subset of ATMs that accumulate in eWAT. Macrophages also acquired this characteristic in coculture with 3T3-L1 adipocytes. RP105 knockout (KO) and MD-1 KO mice had less HFD-induced adipose tissue inflammation, hepatic steatosis, and insulin resistance compared with wild-type (WT) and TLR4 KO mice. Finally, the saturated fatty acids, palmitic and stearic acids, are endogenous ligands for TLR4, but they did not activate RP105/MD-1. Thus, the RP105/MD-1 complex is a major mediator of adipose tissue inflammation independent of TLR4 signaling and may represent a novel therapeutic target for obesity-associated metabolic disorders. ***Diabetes* 61:1199–1209, 2012**

From the [1]Department of Immunobiology and Pharmacological Genetics, Graduate School of Medicine and Pharmaceutical Science for Research, University of Toyama, Toyama, Japan; the [2]Department of First Internal Medicine, Graduate School of Medicine and Pharmaceutical Science for Research, University of Toyama, Toyama, Japan; the [3]Department of Diagnostic Pathology, Graduate School of Medicine and Pharmaceutical Science for Research, University of Toyama, Toyama, Japan; the [4]Department of Clinical Pharmacology, Graduate School of Medicine and Pharmaceutical Science for Research, University of Toyama, Toyama, Japan; the [5]Department of Cardiovascular Medicine, Institute of Health Biosciences, The University of Tokushima Graduate School, Tokushima, Japan; the [6]Department of Molecular Medicine and Metabolism, Medical Research Institute, Tokyo Medical and Dental University, Tokyo, Japan; the [7]Department of Urology, Institute of Health Biosciences, The University of Tokushima Graduate School, Tokushima, Japan; the [8]Laboratory of Host Defense, WPI Immunology Frontier Research Center, Osaka University, Osaka, Japan; the [9]Division of Infectious Genetics, Department of Microbiology and Immunology, The Institute of Medical Science, The University of Tokyo, Tokyo, Japan; the [10]Department of Cardio-Diabetes Medicine, Institute of Health Biosciences, The University of Tokushima Graduate School, Tokushima, Japan; and the [11]Toyama Prefectural Institute for Pharmaceutical Research, Toyama, Japan.
Corresponding authors: Yoshinori Nagai, ynagai@med.u-toyama.ac.jp, and Kiyoshi Takatsu, takatsuk@med.u-toyama.ac.jp.
Received 24 August 2011 and accepted 3 February 2012.
DOI: 10.2337/db11-1182
This article contains Supplementary Data online at http://diabetes.diabetesjournals.org/lookup/suppl/doi:10.2337/db11-1182/-/DC1.
Y.W., T.N., and Y.N. contributed equally to this work.
Y.N. and K.Ta. are both senior authors.
T.N. is currently affiliated with the R&D Center, Ikeda Mohando, Toyama, Japan.
Y.H. is currently affiliated with the Department of Pediatrics, Graduate School of Medicine, The University of Tokyo, Tokyo, Japan.

Obesity is associated with chronic low-grade inflammation characterized by increased pro-inflammatory cytokines and infiltration of macrophages within adipose tissue (1), leading to insulin resistance (2). Although several inflammatory mediators and cell types promote these processes, precise roles of the immune system are not fully understood. Most of the infiltrated adipose tissue macrophages (ATMs) in obese adipose tissue are CD11c-positive inflammatory M1 macrophages responsible for the development of adipose tissue inflammation, which is countered by CD206-positive anti-inflammatory M2 macrophages (3,4).

Pattern recognition receptors (PRRs) such as Toll-like receptors (TLRs) quickly recognize pathogenic agents called pathogen-associated molecular patterns (5). The TLR4/myeloid differentiation protein (MD)-2 complex is indispensable for lipopolysaccharide (LPS) recognition (6,7). TLR4 requires two important adaptor molecules, myeloid differentiation factor 88 (MyD88) and TIR-domain-containing adaptor-inducing interferon-β (TRIF), to transmit its downstream signaling (5). A TLR4 homolog, radioprotective 105 (RP105), forms a complex with MD-1 (8,9). RP105 or MD-1 knockout (KO) mice show reduced proliferative responses to LPS in B cells and are impaired in hapten-specific antibody production against LPS (10–12), suggesting that the RP105/MD-1 complex cooperates with the TLR4/MD-2 complex in LPS responses. RP105/MD-1 also is expressed on macrophages (12). However, roles for RP105/MD-1 in chronic inflammation–associated metabolic disorders have not been suspected.

PRRs also can sense endogenous ligands called danger-associated molecular patterns. These include intracellular molecules such as fatty acids (FAs), heat shock proteins, and host nucleic acids, as well as extracellular components, such as hyaluronan and proteoglycans (13). These molecules can ligate PRRs, leading to activation of proinflammatory pathways and cytokine secretion. This often is referred to as "sterile" inflammation (14).

Adipose tissue–derived saturated free FAs may stimulate TLR4 and promote adipose tissue inflammation and insulin resistance (15–17). The Nlrp3 (nucleotide-binding domain, leucine-rich repeats containing family, pyrin domain-containing-3) inflammasome senses obesity-associated FAs and contributes to obesity-induced inflammation and insulin resistance (18,19). Double-stranded RNA-dependent protein kinase can sense FAs from nutrients as well as endoplasmic reticulum stress and plays critical roles in regulating insulin action and metabolism (20). Of interest, the G-protein–coupled receptor 120 recognizes unsaturated

omega-3 FAs (docosahexaenoic acid and eicosapentaenoic acid) and mediates insulin sensitizing by suppressing macrophage-induced inflammation (21). However, it remains unclear whether RP105/MD-1 has a role in sensing obesity-related natural ligand or whether the complex participates in immune responses leading to diet-induced chronic inflammation and insulin resistance.

We now report that RP105 or MD-1 KO mice were protected from high-fat diet (HFD)-induced obesity, hepatic steatosis, insulin resistance, and adipose tissue inflammation. RP105/MD-1 was expressed on macrophages in the stromal vascular fraction (SVF) of epididymal white adipose tissue (eWAT). RP105 mRNA expression was significantly increased in the visceral adipose tissue (VAT) of obese subjects. An HFD and coculture with adipocytes dramatically increased the expression of RP105 by macrophages. Endogenous TLR4 ligands, palmitic and stearic acids, did not stimulate RP105/MD-1. Therefore, the RP105/MD-1 receptor complex contributes in unique ways to diet-induced obesity and related inflammatory responses.

RESEARCH DESIGN AND METHODS

Mice. C57BL/6 mice were purchased from Japan SLC (Hamamatsu, Japan) and were used at 10 weeks of age. Mice were fed an HFD containing 60% fat (Research Diet, New Brunswick, NJ) or a standard diet containing 10% fat starting at 10 weeks of age for 12 weeks. Male mice were maintained in microisolator cages under specific pathogen-free conditions with a 12-h light/12-h dark cycle in the animal facility of University of Toyama and given free access to food and water. All experiments were performed according to the guidelines for the care and treatment of experimental animals at the University of Toyama.

Reagents. LPS from *Escherichia coli* O55:B5, palmitic, stearic, and lauric acids were purchased from Sigma-Aldrich (St. Louis, MO).

Human study. A total of 18 Japanese male patients with urological diseases who received surgery in Tokushima University Hospital were recruited in this study (Supplementary Table 1). Adipose tissue around the kidney or prostate was obtained as VAT samples. Subcutaneous adipose tissue (SAT) samples were obtained from the abdominal walls during urological surgery. This study protocol was approved by the ethics committee on human research of the University of Tokushima Graduate School and University of Toyama.

Metabolic measurements. Serum total cholesterol and alanine transaminase (ALT) were measured by Reflotron-plus (Roche Diagnostics, Mannheim, Germany). The glucose tolerance test (GTT) was performed by intraperitoneally injecting 1 g glucose/kg. For the insulin tolerance test (ITT), the mice were injected with 0.75 units of human insulin/kg i.p. (Eli Lilly, Indianapolis, IN). Blood glucose was measured by NIPRO FreeStyle FLASH (NIPRO, Osaka, Japan), and serum insulin was measured by an enzyme-linked immunosorbent assay kit (Shibayagi, Shibukawa, Japan).

Measurement of Vo_2, Vco_2, and respiratory quotient. Mice were placed in standard metabolic cages (model MK5000RQ; Muromachikikai, Tokyo, Japan) with an airflow of 0.5 L/min. Oxygen consumption (Vo_2) and carbon dioxide production (Vco_2) were measured during 3 consecutive days (three dark cycles and two light cycles). Respiratory quotient (R_Q) was calculated as a ratio of Vco_2 to Vo_2.

Isolation of adipocytes and SVF from eWAT. Mice were fasted for 12 h before dissection. Isolation of adipocytes and SVF was performed as described previously (4).

Flow cytometry analysis. The cells (1×10^5) were incubated with anti-mouse FcγR (2.4G2) to block binding of the labeled antibodies to FcγR. After 15 min, the cells were stained with predetermined optimal concentrations of the respective antibodies. 7-Amino-actinomycin D (BD Bioscience, San Diego, CA) was used to exclude dead cells. Flow cytometry analyses were conducted on a FACSCanto (Becton Dickinson, Mountain View, CA), and the data were analyzed with Flowjo software (Treestar, San Carlos, CA). The information for antibodies is listed in Supplementary Table 2.

Cell culture. RAW264.7 cells (RIKEN BioResource Center, Tsukuba, Japan) and 3T3-L1 cells (American Type Culture Collection, Manassas, VA) were maintained with DMEM containing 10% fetal calf serum and antibiotics and incubated at 37°C in a humidified 5% CO_2. 3T3-L1 cells were differentiated based on a standard protocol (22). Bone marrow–derived macrophages (BMMs) were differentiated into M1 and M2 macrophages as described previously (23).

Coculture of adipocytes and macrophages. Coculture of 3T3-L1 cells and macrophages was performed as described previously (17). RAW264.7 cells were cocultured with the 3T3-L1 cells in the absence or presence of pioglitazone (Funakoshi, Tokyo, Japan) for 24 h.

Real-time quantitative PCR. Total RNA was isolated with an RNeasy mini kit (Qiagen, Hilden, Germany) or TRIzol Reagent (Invitrogen, Carlsbad, CA). RNA was reverse transcribed with a TaqMan Reverse Transcription Reagents (Applied Biosystems, Carlsbad, CA). Real-time quantitative PCR (RT-qPCR) was performed with a TaqMan Gene Expression Master Mix (Applied Biosystems) and analyzed with an Mx3000P (Agilent Technologies, Santa Clara, CA). Relative transcript abundance was normalized for that of Hprt mRNA. The information for primers is listed in Supplementary Table 3.

Immunoprecipitation and Western blot analysis. The immunoprecipitation for RP105 was performed by using anti-RP105 (RP/14) (24). To detect RP105 by Western blotting, the anti-RP105 (0.5 μg/mL) (ProSci, Poway, CA) and horseradish peroxidase–conjugated anti-rabbit IgG (Cell Signaling, Beverly, MA) were used. Anti-actin was purchased from Sigma-Aldrich. The reactive bands were visualized by ECL Plus (GE Healthcare, Little Chalfont, Bucks, U.K.).

Immunohistochemistry analysis. Portions of the liver and eWAT were excised and immediately fixed with 4% formaldehyde at room temperature. Paraffin-embedded tissue sections were cut into 4-mm slices and placed on slides. CD11c staining was performed as described previously (4). The sections were incubated with anti–Mac-2 (macrophage surface glycoproteins binding to galectin-3), anti–MD-1 (MD113), or anti-RP105 (ProSci) for 1 h and then with ready-to-use polymered secondary antibodies for rat or rabbit monoclonal antibodies with peroxydase (Envision-PO; Dako, Glostrup, Denmark) for 1 h. Bound antibodies were detected with 3,3′-diaminobenzidine. Sections were counterstained with hematoxylin.

Statistical analysis. Statistical significance was evaluated by one-way ANOVA followed by a post hoc Tukey test. $P < 0.05$ was considered statistically significant.

RESULTS

RP105 expression dramatically increases in the adipose tissue from HFD-fed mice and obese subjects. Our initial studies evaluated the expression of genes encoding RP105/MD-1, TLRs, MD-2, and components involved in TLR signaling in the eWAT from WT mice fed with a normal diet (ND) or an HFD (Fig. 1*A*). HFD treatment markedly increased the expression of RP105 mRNA by 13-fold. The expression of MD-1, TLR1, TLR7, TLR8, and TLR9 mRNA also was increased by HFD, whereas the expression of TLR4 and MD-2 mRNA was not affected. The MyD88 and TRIF are critical adaptor molecules for TLR4 signaling (5) but are not involved in RP105 signaling (data not shown). MyD88 and TRIF mRNA, as well as TLR4 mRNA, were not increased by an HFD in eWAT (Fig. 1*A*). RP105 and MD-1 mRNAs also were significantly increased in other WAT depots, such as subcutaneous and retroperitoneal WAT, by an HFD (Supplementary Fig. 1). Levels of TLR4 mRNA in retroperitoneal adipose tissue were slightly increased by an HFD. HFD also increased RP105 mRNA in the liver, brown adipose tissue, and skeletal muscle by 1.6-, 3-, and 1.7-fold, respectively (Supplementary Fig. 2). In addition, the expression of RP105 and MD-1 mRNA in the spleen and bone marrow was not significantly affected by an HFD. Expression of TLR4, MD-2, MyD88, and TRIF in these tissues was not significantly affected by an HFD.

To test the clinical relevance of data generated from mouse models, we examined RP105 and MD-1 mRNA expression in human adipose tissue. Linear regression analyses showed a positive correlation between RP105 mRNA levels and BMI in the VAT but not the SAT (Fig. 1*B*). RP105 mRNA expression was increased in the VAT but not the SAT of obese subjects relative to nonobese subjects (Fig. 1*C*). In contrast, MD-1 mRNA expression was significantly increased in the SAT but not the VAT of obese subjects (Supplementary Fig. 3).

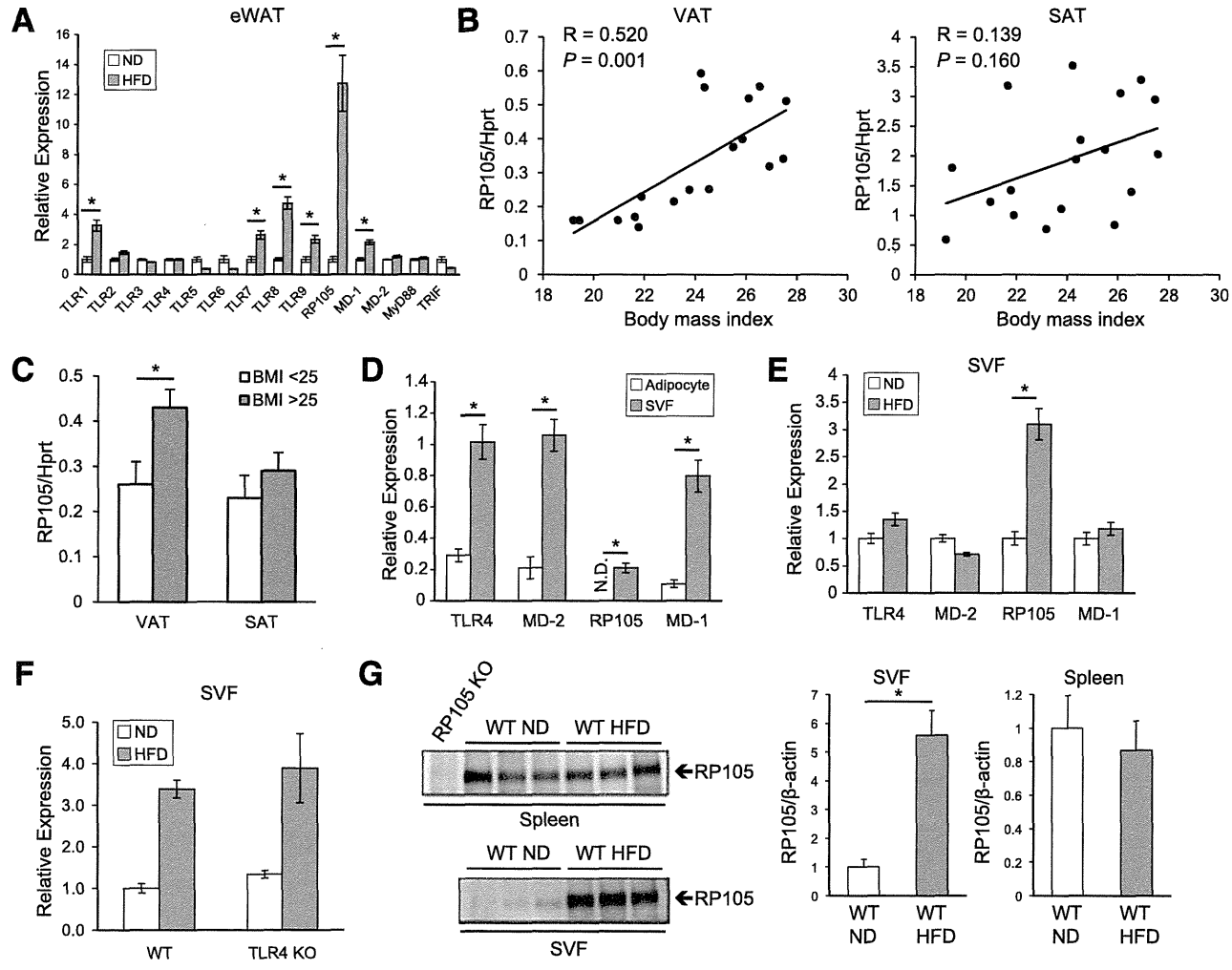

FIG. 1. RP105 and MD-1 expression in mouse and human adipose tissues. *A*: RT-qPCR of TLRs, RP105/MD-1, MD-2, MyD88, and TRIF mRNA in the eWAT from WT fed with an ND or HFD for 12 weeks (n = 8 per group). Data are presented relative to the expression in ND-fed mice, set as 1. Data are shown as means ± SE. *P < 0.05 vs. ND. *B*: Linear regression analysis of the correlation between adipose RP105 mRNA expression and BMI. *C*: RP105 mRNA expression of the human adipose tissue of nonobese (BMI <25 kg/m^2; n = 11) and obese (BMI >25 kg/m^2; n = 7) subjects. Data are shown as means ± SE. *P < 0.05. *D*: RT-qPCR of TLR4, MD-2, RP105, and MD-1 mRNA in adipocytes and SVF from WT mice on an ND (n = 8 per group). Data are shown as means ± SE. *P < 0.05 vs. adipocyte. N.D., not detected. *E*: RT-qPCR of TLR4, MD-2, RP105, and MD-1 mRNA in SVF from WT mice on an ND or HFD for 12 weeks (n = 8 per group). Data are presented relative to the expression in the ND, set as 1. Data are shown as means ± SE. *P < 0.05 vs. ND. *F*: RT-qPCR of RP105 mRNA in SVF from WT or TLR4 KO mice fed with an ND or HFD for 12 weeks (n = 7 per group). Data are presented relative to the expression in WT mice fed with an ND, set as 1. Data are shown as means ± SE. *G*: Immunoprecipitation analysis of RP105 in lysates of spleen (2 × 10^7 cells/lane) or SVF (2 × 10^6 cells/lane) from WT mice on an ND or HFD for 12 weeks. Data are presented as means ± SE normalized to β-actin expression (bar graphs). *P < 0.05 vs. WT ND.

To determine the nature of RP105-bearing cells in eWAT, we isolated adipocytes and the SVF from the eWAT of WT mice (Fig. 1*D*). In adipocytes, MD-1, TLR4, and MD-2 mRNA were expressed, whereas RP105 mRNA was not detected. The SVF expressed all the tested genes, but the level of RP105 mRNA was lower than those of others. In SVF, only RP105 was increased by an HFD (Fig. 1*E*). In addition, this change was independent of TLR4 signaling, as it was present in KO mice lacking TLR4 (Fig. 1*F*). Likewise, RP105 protein levels were increased in obese mice compared with lean mice (Fig. 1*G*). This change was not detected in the spleen. These results indicate that the expression of RP105 is associated with diet-induced obesity.

The RP105/MD-1 complex is expressed in ATMs. We then traced the expression of RP105 and MD-1 in SVF cells. Approximately 40% of the SVF cells from ND-fed mice were composed of CD45$^+$ cells, and the percentage increased to ~55% by HFD (Fig. 2*A*). In contrast, an HFD decreased the percentage of CD45$^-$ cells. RP105 and MD-1 were seen on CD45$^+$ but not CD45$^-$ cells in ND-fed mice (Fig. 2*B*). Those leukocytes were heterogeneous with respect to RP105 and MD-1 densities, and the percentages of RP105- and MD-1–bearing cells increased by HFD. The TLR4/MD-2 complex was not displayed by either CD45$^+$ or CD45$^-$ cells. The staining intensity of RP105 correlated with that of MD-1 (Fig. 2*C*). There was good correlation between transcript expression and flow cytometry results (Supplementary Fig. 4). Of interest, CD45$^-$ cells had TLR4 and MD-2 mRNA, and an HFD increased MD-2 mRNA in CD45$^-$ cells by approximately threefold.

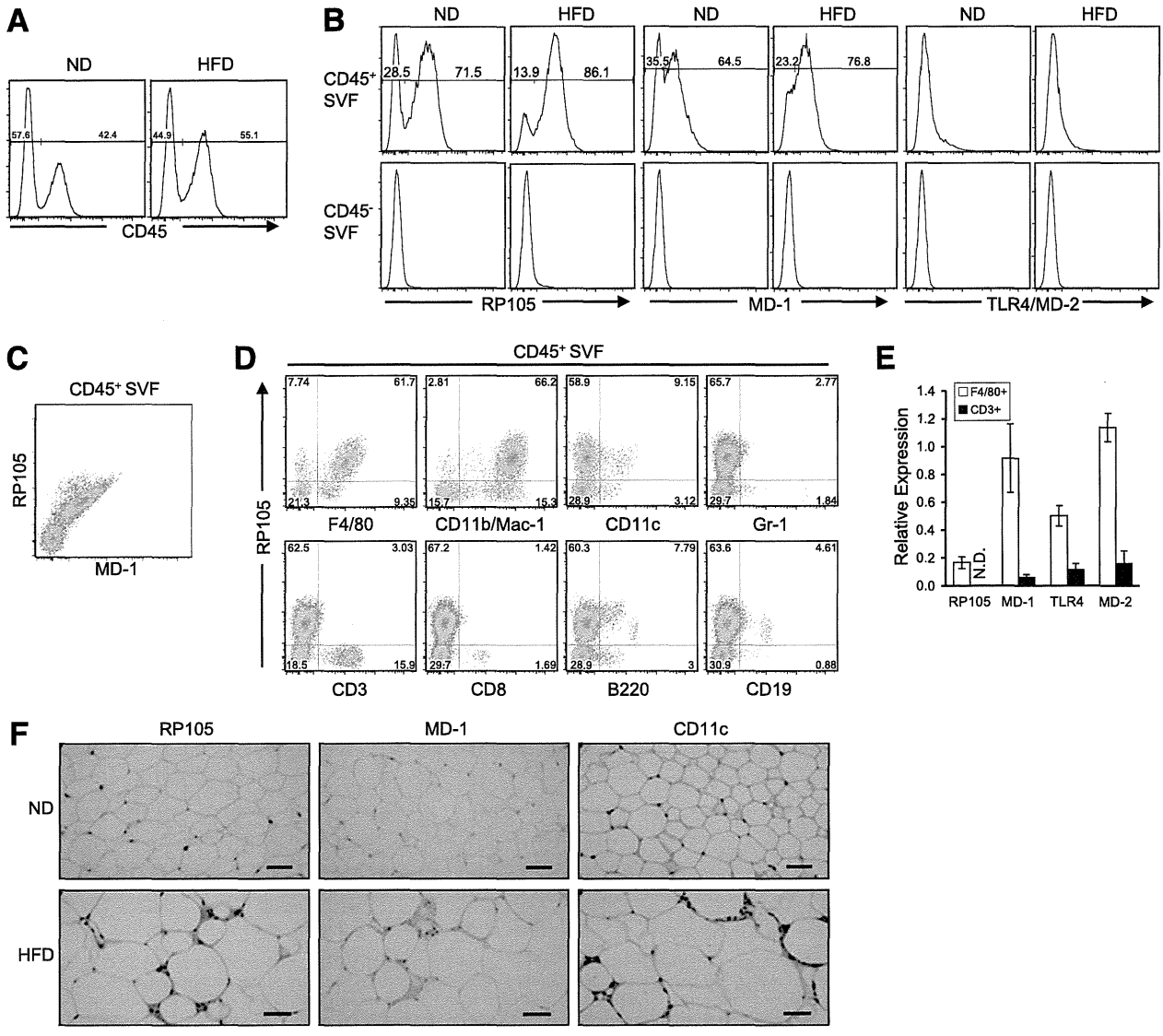

FIG. 2. ATMs are major RP105/MD-1-expressing cells in SVF. *A*: Flow cytometry analysis of CD45 expression on SVF cells from WT mice on an ND or HFD for 12 weeks. *B*: Flow cytometry analysis of RP105, MD-1, and TLR4/MD-2 expression on $CD45^+$ or $CD45^-$ SVF cells from WT mice on an ND or HFD for 12 weeks. *C*: Flow cytometry analysis of RP105 and MD-1 expression on $CD45^+$ SVF cells from WT mice on an ND. *D*: Flow cytometry analysis of $CD45^+$ SVF cells from WT mice on an ND. *E*: RT-qPCR of RP105, MD-1, TLR4, and MD-2 mRNA in $F4/80^+$ or $CD3^+$ SVF cells from WT mice on an ND. Data are shown as means ± SE. N.D., not detected. *F*: Representative histological images of eWAT from WT mice on an ND or HFD for 12 weeks stained with RP105, MD-1, and CD11c. Scale bars, 50 μm (ND) and 100 μm (HFD). All data are representative of at least two independent experiments. (A high-quality digital representation of this figure is available in the online issue.)

Additional flow cytometry analyses revealed that a majority of the RP105-expressing $CD45^+$ cells were $F4/80^+$ and $CD11b/Mac\text{-}1^+$ (Fig. 2*D*). Some RP105-expressing cells were CD11c, B220, and CD19 positive. $CD8^+$ T cells have been reported to promote the recruitment and activation of macrophages in adipose tissue (25). However, $CD3^+$ and $CD8^+$ cells did not have detectable RP105 (Fig. 2*D*). $CD3^+$ cells had no RP105 and low MD-1 mRNA (Fig. 2*E*). In addition, RP105 and MD-1 were made by $CD11b/Mac\text{-}1^+$ and $CD19^+$ cells but not $CD3^+$ cells in spleen cells of WT animals (Supplementary Fig. 5*A* and *B*). RP105 and MD-1 were predominantly expressed in ATM clusters in eWAT from HFD-fed mice (Fig. 2*F*). These RP105-/MD-1–positive cells also stained positive for CD11c. It is clear from these findings that majority of RP105-/MD-1–expressing SVF cells is ATMs.

Expression of RP105 and MD-1 on M1 macrophages reflects differentiation and is regulated by HFD and adipocytes. Additional information about RP105/MD-1 expression was obtained by examination of M1 and M2 macrophage subsets (Fig. 3*A*). Differentiated M1 macrophages were strongly positive for RP105 and MD-1 as well as tumor necrosis factor (TNF)-α and inducible nitric oxide synthase, representative M1 markers. MD-2 mRNA also was significantly increased by M1 differentiation. In contrast to the expression of arginase 1 and Mgl2 mRNA, the levels of RP105 and MD-1 mRNA in M2 were similar to those in undifferentiated BMMs. TLR4 and MD-2 mRNA were not significantly influenced by M2 differentiation. The RP105/MD-1 complex was detected on M1 and M2 ATMs from ND-fed mice (Fig. 3*B*). Of interest, RP105/MD-1 on

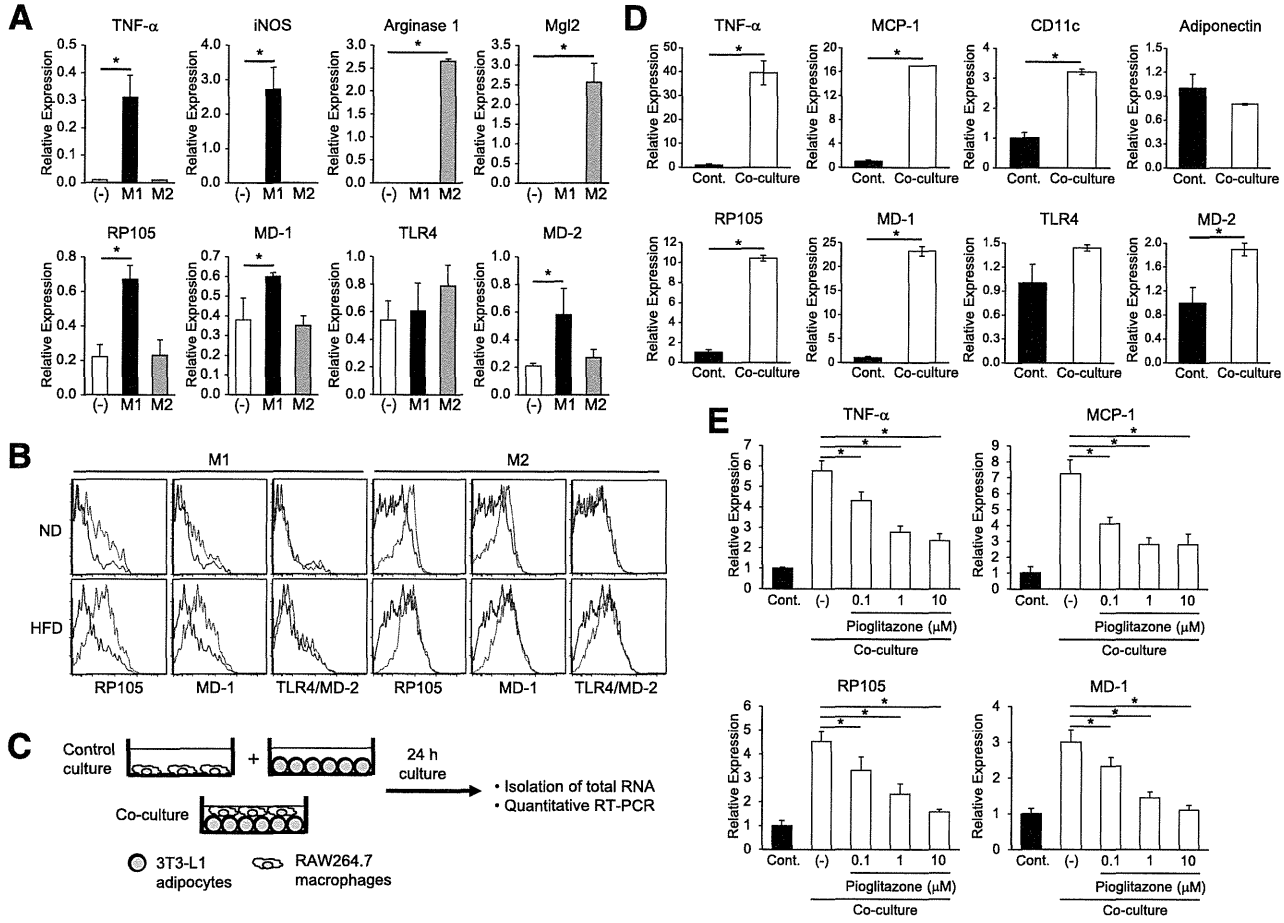

FIG. 3. Expression of RP105 and MD-1 in M1 macrophages is regulated by HFD and adipocytes. *A*: **RT-qPCR of M1 markers (TNF-α and inducible nitric oxide synthase [iNOS]), M2 markers (arginase 1 and Mgl2), RP105, MD-1, TLR4, and MD-2 mRNA in differentiated M1 and M2 macrophages (n = 3 per group). (−), undifferentiated BMMs. *P < 0.05 vs. (−).** *B*: **Flow cytometry analysis of RP105, MD-1, and TLR4/MD-2 expression on M1 and M2 ATMs from WT mice fed with an ND or HFD for 12 weeks (blue lines, isotype control antibodies). All data are representative of at least three independent experiments.** *C*: **Illustration of the coculture system.** *D*: **RT-qPCR of TNF-α, MCP-1, CD11c, adiponectin, RP105, MD-1, TLR4, and MD-2 mRNA in the control and cocultured cells (n = 3 per group). As the control, the equal numbers of each cell were cultured separately and mixed after harvest. Data are presented relative to the expression in the control culture, set as 1. *P < 0.05 vs. control culture.** *E*: **RT-qPCR of TNF-α, MCP-1, RP105, and MD-1 mRNA in the control and cocultured cells with or without pioglitazone (n = 3 per group). Data are presented relative to the expression in the control culture, set as 1. (−), coculture without pioglitazone. *P < 0.05 vs. coculture without pioglitazone. Data are shown as means ± SE (*A*, *D*, and *E*). All data are representative of at least three independent experiments.**

M1 but not M2 ATMs was upregulated by an HFD. The TLR4/MD-2 complex was not displayed on ATMs from both ND- and HFD-fed mice.

To understand molecular mechanisms underlying HFD-induced upregulation of RP105/MD-1 on M1 ATMs, we prepared a coculture system composed of 3T3-L1 adipocytes and macrophages (Fig. 3*C*). Using this approach, a previous study determined that saturated FAs and TNF-α in a paracrine loop could exacerbate adipose tissue inflammation (15). We observed increased expression of TNF-α, monocyte chemoattractant protein (MCP)-1, and CD11c and decreased expression of adiponectin in the cocultured cells (Fig. 3*D*). In parallel with the upregulation of TNF-α and CD11c, RP105 and MD-1 were markedly increased in the cocultured cells compared with cells in control cultures. Because 3T3-L1 cells did not express RP105 and MD-1 mRNA, macrophages were responsible for this change (data not shown). In addition, this increase was independent of TLR4 (Supplementary Fig. 6). We also observed increased expression of TLR4 and MD-2, but these changes were smaller than those of RP105 and MD-1 (Fig. 3*D*). A peroxisome proliferator–activated receptor-γ agonist pioglitazone treatment of HFD-fed WT mice decreased M1 markers and increased M2 markers in eWAT (4). Pioglitazone stimulation decreased RP105 and MD-1 mRNA, as well as TNF-α and MCP-1 mRNA induced by the coculture in a dose-dependent manner (Fig. 3*E*). Collectively, RP105 and MD-1 are associated with differentiation and responsible for activation of M1 macrophages.

RP105 KO and MD-1 KO mice have increased energy expenditure and are protected from HFD-induced obesity and hepatic steatosis. The above observations led us to analyze RP105 KO and MD-1 KO mice in the development of obesity and insulin resistance, comparing them with WT and TLR4 targeted animals. RP105 KO and MD-1 KO mice gained significantly less weight than WT and TLR4 KO mice on an HFD, whereas no significant differences were found in body weights on an ND (Fig. 4*A*). Representative photos and magnetic resonance imaging revealed decreased fat masses in RP105 KO and MD-1 KO

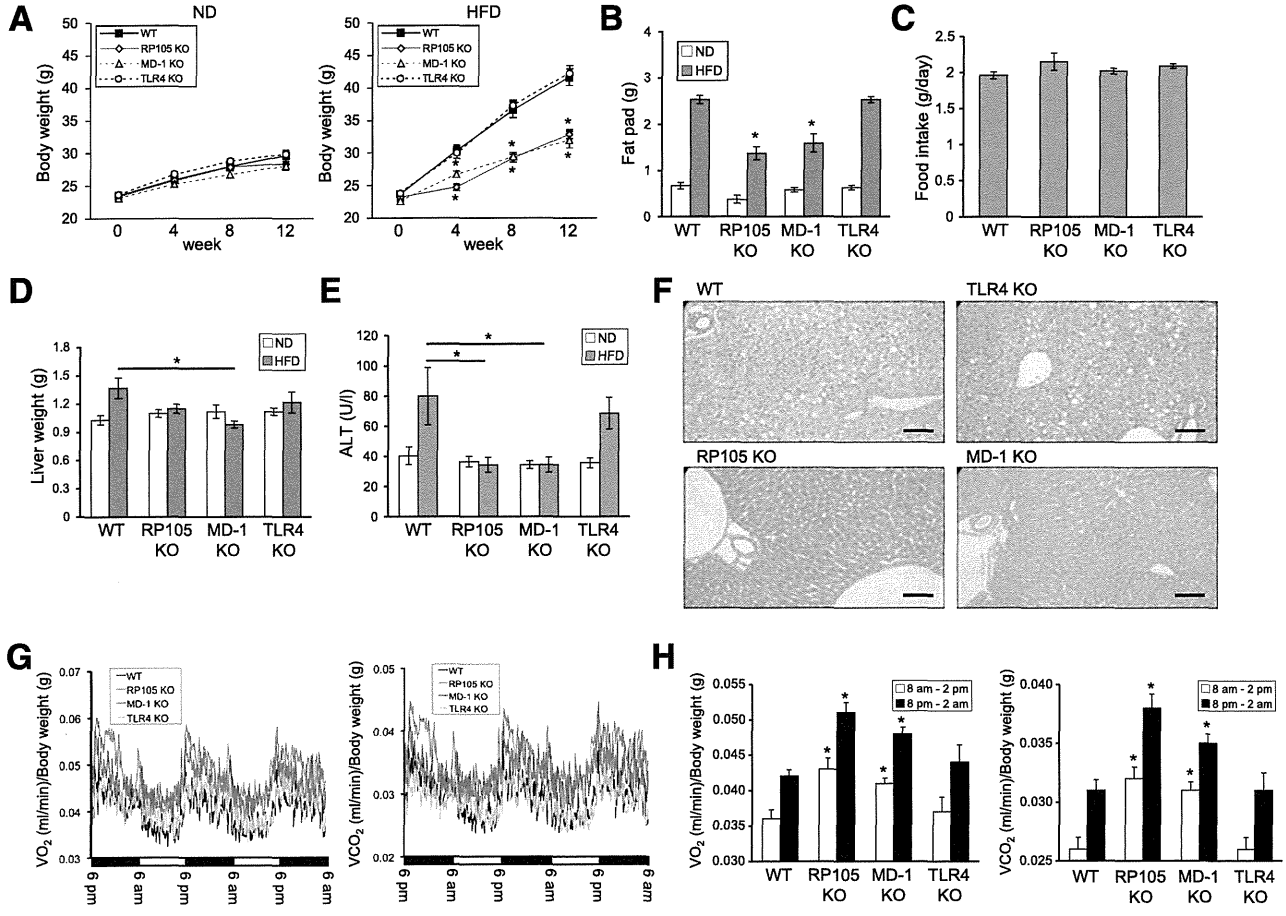

FIG. 4. RP105 KO and MD-1 KO mice with increased energy expenditure are protected from HFD-induced obesity and hepatic steatosis. *A*: Body weight changes of WT, RP105 KO, MD-1 KO, and TLR4 KO mice fed with an ND or HFD (n = 12 per group). *B*: Fat-pad weights of WT, RP105 KO, MD-1 KO, and TLR4 KO mice fed with an ND or HFD for 12 weeks (n = 12 per group). *C*: Food intake was measured for WT, RP105 KO, MD-1 KO, and TLR4 KO mice fed with an HFD for 12 weeks (n = 12 per group). *D*: Liver weights of WT, RP105 KO, MD-1 KO, and TLR4 KO mice fed with an ND or HFD for 12 weeks (n = 12 per group). *E*: Serum ALT levels were measured for 12-h fasting mice fed with an ND or HFD for 12 weeks (n = 12 per group). *F*: Representative images of hematoxylin and eosin–stained sections of livers from WT, RP105 KO, MD-1 KO, and TLR4 KO mice fed with an HFD for 12 weeks. Scale bars, 200 μm. *G*: Oxygen consumption (V_{O_2}) and carbon dioxide consumption (V_{CO_2}) were measured for WT, RP105 KO, MD-1 KO, and TLR4 KO mice fed with an HFD for 12 weeks (n = 6 per group). Data are shown as means. *H*: The data from 8 A.M. to 2 P.M. or 8 P.M. to 2 A.M. in *G* were calculated and shown as bar graphs. Data are shown as means ± SE (*A–E* and *H*). *$P < 0.05$ vs. WT (*A*, *B*, *D*, *E*, and *H*). (A high-quality digital representation of this figure is available in the online issue.)

mice on the HFD (Supplementary Fig. 7*A* and *B*). Fat-pad weights were similar in WT and TLR4 KO animals on the HFD but much smaller in RP105 KO and MD-1 KO mice (Fig. 4*B*). Daily food intakes were similar in all groups of mice (Fig. 4*C*).

Chronic exposure of mice to HFD causes hepatic steatosis. In WT mice, this is reflected in increased liver weights and levels of serum ALT (Fig. 4*D* and *E*). The latter response was abrogated in *Rp105* and *Md-1* gene–targeted animals. HFD induced macrovesicular steatosis in WT and TLR4 KO but not RP105 or MD-1 KO mice (Fig. 4*F*).

We further found no significant differences in locomotor activity in these mice (Supplementary Fig. 8*A*). RQ fluctuated between 0.70 and 0.75 in all groups of mice maintained on the HFD (Supplementary Fig. 8*B*). O_2 and CO_2 consumption were significantly increased through light and dark phases in RP105 KO and MD-1 KO mice, whereas these measurements were similar in WT and TLR4 KO mice (Fig. 4*G* and *H*). These data clearly demonstrated that RP105 KO and MD-1 KO mice are protected from HFD-induced obesity and hepatic steatosis, and energy expenditure is increased when RP105 and MD-1 are nonfunctional.

RP105 KO and MD-1 KO mice are protected from HFD-induced hypercholesterolemia and insulin resistance. All gene-targeted animals had reduced fasting serum cholesterol levels on the HFD (Fig. 5*A*). Chronic exposure to HFD increased fasting glucose and insulin levels in WT and TLR4 KO but not RP105 and MD-1 KO mice (Fig. 5*B* and *C*). The HFD caused insulin resistance and impaired glucose tolerance in WT mice, whereas the KO mice seemed to be more insulin sensitive and to have better glucose tolerance (Fig. 5*D* and *E*). Insulin sensitivities of MD-1 KO and TLR4 KO but not RP105 KO mice significantly improved compared with WT mice (Fig. 5*F*, *left*). Significant differences between WT and the KO mice were not observed in the GTT (Fig. 5*F*, *right*).

HFD-induced macrophage infiltration and adipose tissue inflammation are attenuated in RP105 KO and MD-1 KO mice. The improved insulin action in RP105- or MD-1–deficient mice led us to investigate cell subsets in

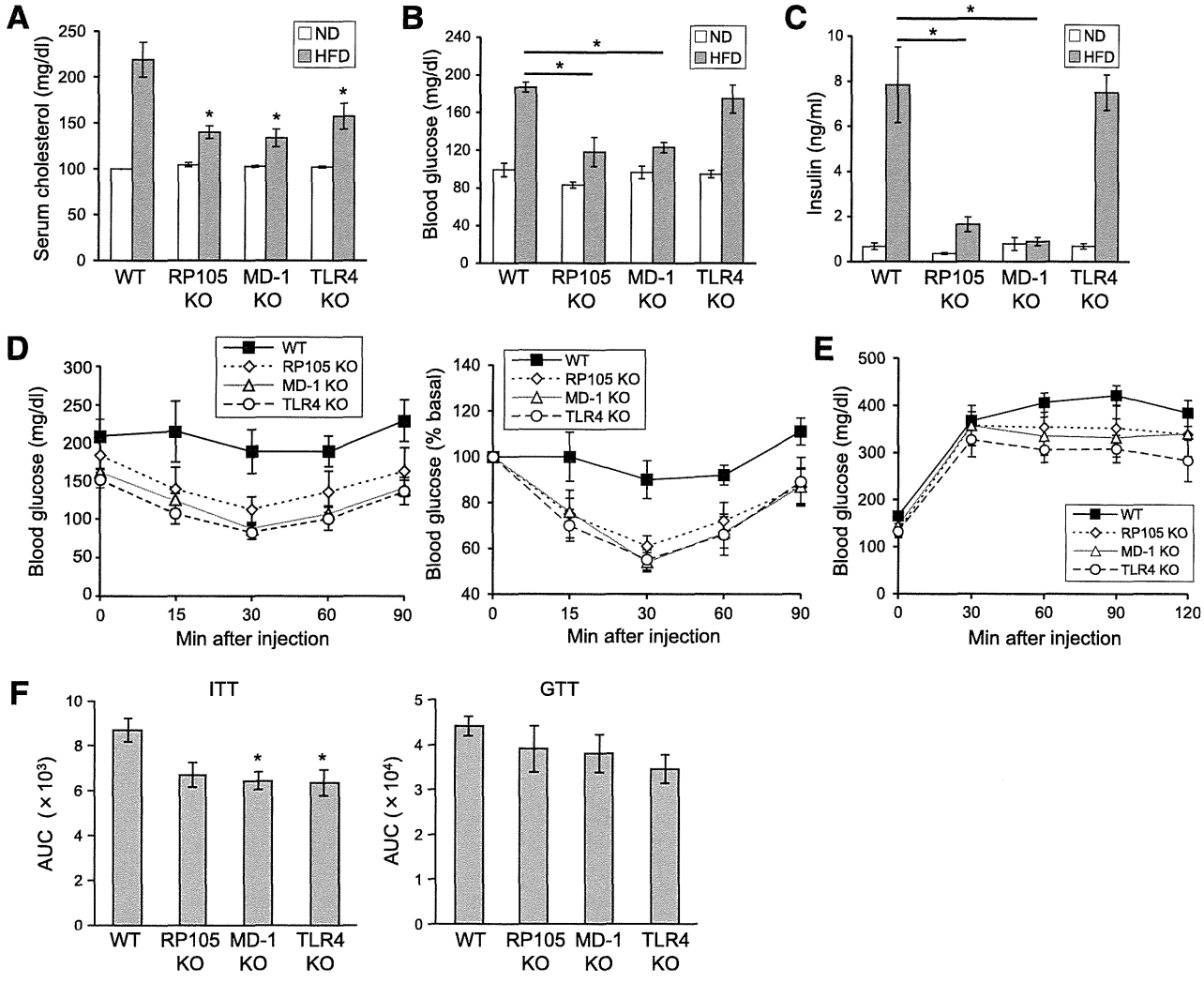

FIG. 5. RP105 KO and MD-1 KO mice are protected from HFD-induced hypercholesterolemia and insulin resistance. *A*: Serum cholesterol levels were measured for 12-h fasting mice fed with an ND or HFD for 12 weeks (n = 12 per group). *B* and *C*: Serum glucose (*B*) and insulin (*C*) levels were measured after a 12-h fasting in mice fed with an ND or HFD for 12 weeks (n = 12 per group). *D*: An ITT was performed after 3 h of fasting in mice fed with an HFD for 12 weeks (n = 6 per group). *Left*: Data are presented as absolute values. *Right*: Data are presented relative to the values of 0 min (preinjection), set as 100%. *E*: A GTT was performed after 12 h of fasting in mice fed with an HFD for 12 weeks (n = 6 per group). Data are shown as means ± SE. *F*: Area under the curve (AUC) graphs of ITT (*left*) and GTT (*right*) tests are presented. Data are shown as means ± SE. *P < 0.05 vs. WT.

adipose tissue and assess their expression of inflammatory genes. Compared with WT mice on an HFD, RP105 KO and MD-1 KO mice had severe reductions in the number of SVF cells and F4/80$^+$ cells in eWAT (Fig. 6*A* and *B*). In contrast, adipose tissue from TLR4 KO mice on an HFD exhibited mild reductions in these numbers compared with WT mice. The number of M1 ATMs (F4/80$^+$/CD11c$^+$/CD206$^-$) was markedly reduced in RP105- or MD-1–deficient eWAT compared with WT mice (Fig. 6*C*). M2 ATMs (F4/80$^+$/CD11c$^-$/CD206$^+$) also accumulated in eWAT during obesity (Fig. 6*C*). Their numbers were significantly reduced in RP105 KO, MD-1 KO, and TLR4 KO mice compared with WT mice. An HFD induced a large increase in ATMs, which form a crown-like structure around adipocytes in WT mice (Fig. 6*D*). We observed severe reductions of ATMs in the eWAT of RP105 KO and MD-1 KO mice. TLR4-deficient eWAT showed mild reductions in ATMs compared with WT mice. Expression of inflammatory genes, such as TNF-α, MCP-1, and IKKε, was increased by an HFD compared with an ND in WT and TLR4 KO mice (Fig. 6*E*). TNF-α and MCP-1 mRNAs also were increased by an HFD in subcutaneous and retroperitoneal adipose tissues of WT mice (Supplementary Fig. 1). In contrast, such increases were not observed in the eWAT of RP105 KO and MD-1 KO mice (Fig. 6*E*). Consistent with the reduction in the number of F4/80$^+$ cells and M1 macrophages, expression of F4/80 and CD11c mRNA was decreased in RP105- or MD-1–deficient eWAT fed with an HFD. Adiponectin expression was decreased by an HFD in WT and TLR4 KO mice but not RP105 or MD-1 deficiency. In addition, the lack of RP105/MD-1 did not affect the differentiation of BMMs into M1 subset induced by LPS plus interferon-γ (Fig. 6*F*).

We examined the activity of some of the key signaling molecules involved in adipose tissue inflammation and insulin resistance. To assess the role of Jun NH2-terminal kinase (JNK) (26,27), lysates from eWAT or SVF were

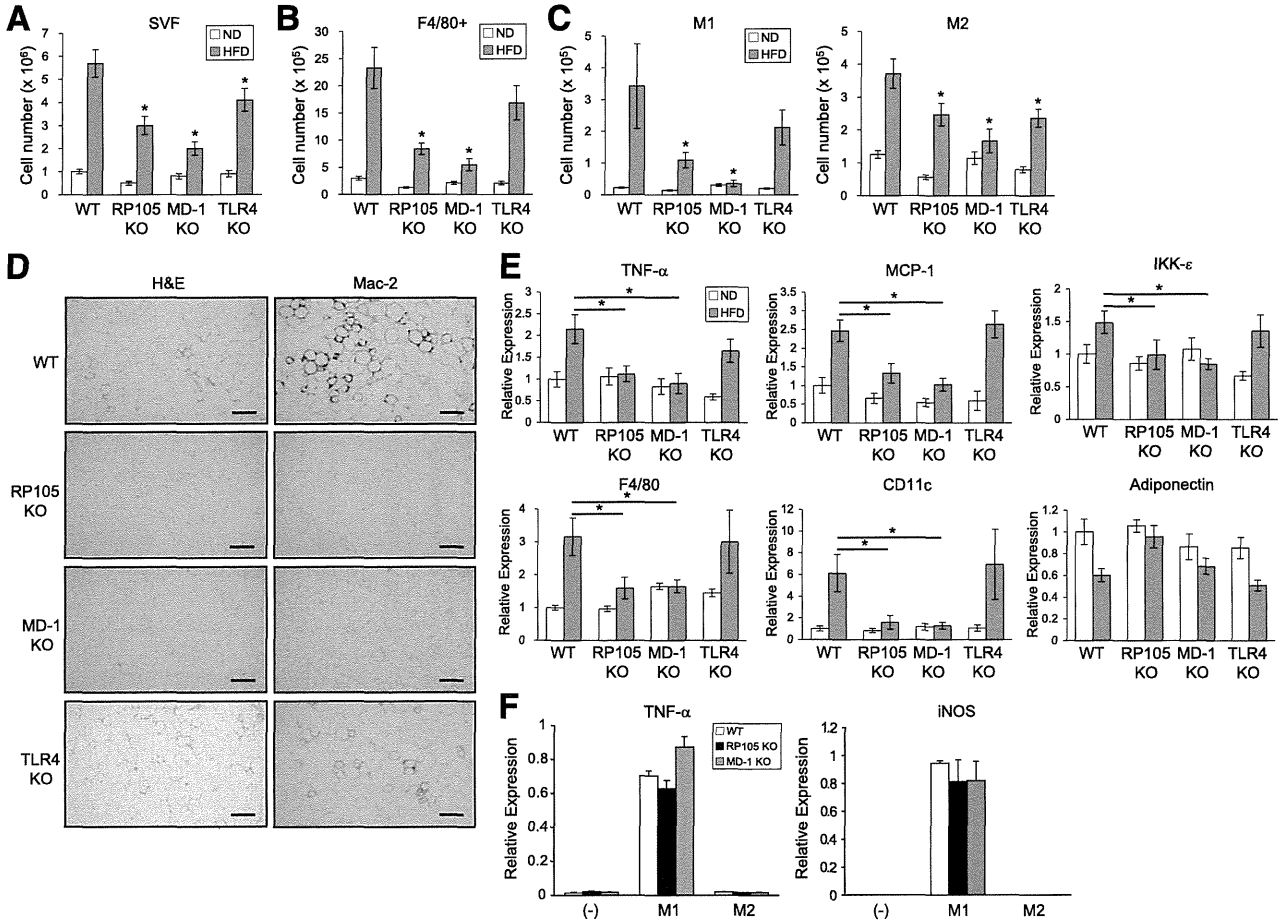

FIG. 6. Obesity-induced macrophage infiltration and adipose tissue inflammation are attenuated in RP105 KO and MD-1 KO mice. *A* and *B*: Cell number of SVF cells (*A*) and F4/80$^+$ cells (*B*) in eWAT from WT, RP105 KO, MD-1 KO, and TLR4 KO mice fed with an ND or HFD for 12 weeks (n = 12 per group). *C*: Cell number of M1 (*left*) and M2 (*right*) macrophages in eWAT from WT, RP105 KO, MD-1 KO, and TLR4 KO mice fed with an ND or HFD for 12 weeks (n = 12 per group). *D*: Representative histological images of eWAT from WT, RP105 KO, MD-1 KO, and TLR4 KO mice fed with an HFD for 12 weeks stained with hematoxylin and eosin (H&E) and Mac-2. Scale bars, 100 μm. *E*: RT-qPCR of TNF-α, MCP-1, IKKε, F4/80, CD11c, and adiponectin mRNA in eWAT from WT, RP105 KO, MD-1 KO, and TLR4 KO mice fed with an ND or HFD for 12 weeks (n = 12 per group). *F*: BMMs from WT, RP105 KO, and MD-1 KO mice were differentiated into M1 or M2 macrophages. After 24 h, expression of M1 markers in the stimulated cells was measured by RT-qPCR. Data are shown as means ± SE (*A–C*, *E*, and *F*). *$P < 0.05$ vs. WT. (A high-quality digital representation of this figure is available in the online issue.)

immunoblotted with a phospho-JNK antibody. We did not observe significant increased phospho-JNK in the eWAT from WT and the KO mice by HFD (Supplementary Fig. 9*A*, *left*). An HFD produced increased phospho-JNK in SVF from WT mice (Supplementary Fig. 9*A*, *right*). Of interest, TLR4 KO but not RP105 KO and MD-1 KO mice exhibited reduced levels of phospho-JNK in SVF by HFD, suggesting that TLR4/MD-2 but not RP105/MD-1 is important for HFD-induced JNK activation. An HFD induced IκBα degradation in SVF from WT but not RP105 KO, MD-1 KO, and TLR4 KO mice, suggesting that nuclear factor (NF)-κB is activated by both TLR4/MD-2 and RP105/MD-1 (Supplementary Fig. 9*B*). IKKε is a direct transcriptional target of NF-κB (28). IKKε phosphorylation was investigated by Western blotting, as a surrogate to assay activation of the kinase. IKKε expression in eWAT was similarly increased after an HFD in WT, RP105 KO, MD-1 KO, and TLR4 KO mice (Supplementary Fig. 9*C*). Of interest, HFD increased levels of phospho-IKKε in eWAT from WT, RP105 KO, and MD-1 KO, but not TLR4 KO, mice, suggesting that IKKε phosphorylation after an HFD is downstream TLR4 but not RP105 signaling.

Because TLRs can regulate inflammatory activation, we wondered whether RP105 KO mice might also be hyporesponsive to acute inflammatory stimuli. LPS injection led to a profound elevation in proinflammatory genes in the SVF (Fig. 7). However, the levels of these genes were not affected by RP105 deficiency. Collectively, the RP105/MD-1 complex contributes to the development of diet-induced chronic, low-grade adipose tissue inflammation.

The RP105/MD-1 complex is not involved in palmitic and stearic acid–induced macrophage activation. Palmitic acid is one of the most abundant saturated FAs in plasma and is substantially elevated by an HFD (29). Furthermore, palmitic acid has been reported to be an endogenous TLR4 ligand (15–17). BSA–palmitic acid, but not BSA alone, increased TNF-α mRNA in WT BMMs (Fig. 8*A*, *upper panel*). TLR4-deficient BMMs showed a lower increase of TNF-α mRNA than WT upon BSA–palmitic acid stimulation. In contrast, WT, RP105-deficient, and MD-1–deficient BMMs

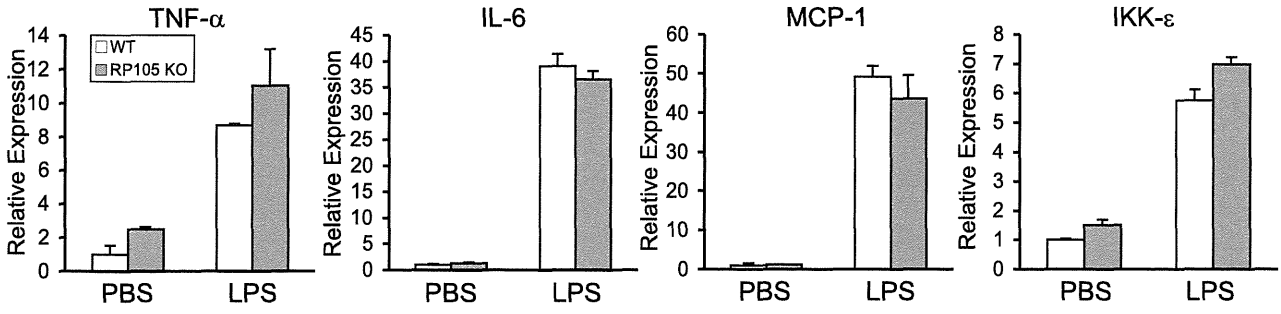

FIG. 7. RP105 does not mediate LPS-induced inflammatory responses in SVF of eWAT. WT and RP105 KO mice (n = 3 per group) were injected with LPS (50 μg/mice) intraperitoneally. After 3 h, SVF was isolated from eWAT and expression of TNF-α, IL-6, MCP-1, and IKKε mRNA was measured by RT-qPCR. Data are presented relative to the expression in PBS-injected WT mice, set as 1. Data are shown as means ± SE. Data are representative of at least two independent experiments.

generated similar levels of TNF-α mRNA in response to BSA–palmitic acid. BMMs also were stimulated with other saturated FAs. Upon 100 μmol/L of BSA–stearic acid stimulation, WT, RP105-deficient, and MD-1–deficient BMMs similarly increased levels of TNF-α mRNA, and this was dependent on TLR4 (Fig. 8*A*, *middle panel*). However, upon 200 μmol/L of BSA–stearic acid stimulation, we did not observe the TLR4 dependency. Although lauric acid induces NF-κB activation in RAW264.7 cells via TLR4 (30), we did not observe significantly increased TNF-α mRNA by BSA–lauric acid in BMMs from WT and all the KO mice (Fig. 8*A*, *lower panel*). Thus, although palmitic and stearic acids activate innate immunity via TLR4/MD-2, a different ligand must be recognized by RP105/MD-1 and be responsible for most of obesity-related inflammation (Fig. 8*B*).

DISCUSSION

Here, we provided evidence that RP105/MD-1 plays a major role in regulating adipose tissue inflammation and metabolic disorders. Many detrimental consequences of an HFD were ameliorated by targeting genes encoding for RP105 or MD-1. TLR4 KO mice showed reduced HFD-induced adipose tissue inflammation (Fig. 6), but our results clearly revealed more requirements of RP105/MD-1 than TLR4/MD-2 in the induction of adipose tissue inflammation and obesity. The higher levels of cell surface and transcript expression of RP105/MD-1 in eWAT might simply reflect the requirements of RP105/MD-1 (Figs. 1–3). As is demonstrated, however, RP105/MD-1 plays unique, TLR4-independent roles in adipose tissue inflammation, and a ligand and signaling pathway of RP105/MD-1 must be different from those of TLR4/MD-2 (Fig. 8*A* and Supplementary Fig. 9). A dietary or endogenous ligand other than palmitic and stearic acids might trigger upregulation of RP105 on macrophages that, in turn, accumulate in adipose tissue. The underlying mechanisms require more investigation, but some aspects are clear.

Both MD-1 and MD-2 are members of the same lipid-recognition family (31), and MD-2 is essential for LPS recognition (7). Crystal structure analyses revealed that MD-1 could recognize lipid-like molecules (32,33). An endogenous ligand for RP105/MD-1 must be something other than palmitic and stearic acids (Fig. 8*A*), inducing adipose tissue inflammation by RP105/MD-1 signaling pathway. Otherwise, it might not necessarily be a saturated FA, since some proteins and other components induce sterile inflammation via TLR4/MD-2. Other lipids or components derived from inflamed tissues might stimulate RP105/MD-1 in adipose tissue inflammation. Identification of ligands that promote adipose tissue inflammation via RP105/MD-1 would be an important achievement.

Although other TLRs have a Toll/interleukin-1 receptor (TIR) domain in the intracellular segment, RP105 has only 11 amino acids in that portion (24). This suggests that RP105 requires another molecule to transmit its signal. In B cells, CD19 regulates RP105 but not TLR4 signaling (34). The MyD88 and TRIF adaptors are involved in TLR4 (5) but not RP105 signaling (data not shown). However, little is known about how RP105 regulates chronic inflammation. The NF-κB pathway plays a crucial role in obesity-associated inflammation. HFD activates NF-κB in fat and liver and increases IKKε expression in M1 macrophages (28). IKKε KO mice do not gain weight on an HFD with increased energy expenditure (28). In addition, IKKε KO mice are protected from diet-induced hepatic steatosis, macrophage infiltration into adipose tissue, and increased expression of inflammatory genes in eWAT. The similarities between these changes and ones we attributed to RP105/MD-1 are intriguing. However, although both TLR4 and RP105 are required for HFD-induced NF-κB activation (Supplementary Fig. 9*B*), IKKε may be activated in the downstream of TLR4 but not the RP105 pathway by HFD (Supplementary Fig. 9*C*). In addition, TLR4 but not RP105 may activate JNK pathway in obese mice (Supplementary Fig. 9*A*). Thus, RP105 shares some signaling pathways with TLR4 but must have distinct ones from TLR4.

Levels of RP105 mRNA in SVF and macrophages were dramatically increased by HFD and coculture with adipocytes, respectively. We did not record similar changes in spleen, bone marrow, or even other immune cells in eWAT (data not shown). This raises the possibility of a self-amplifying, feed-forward mechanism of diet-induced inflammation. Processing or production of an RP105/MD-1 ligand by adipocytes might recruit and activate macrophages that produce cytokines capable of promoting obesity and systemic metabolic changes.

The dramatic changes in metabolic status and inflammation in RP105 KO and MD-1 KO mice we observed might have resulted from lower body weights in these KO mice. However, deletion of some genes prevents inflammation and insulin resistance but not weight gain from an HFD (35–37). Others (16) and we have demonstrated that TLR4 KO mice on an HFD have restored insulin resistance but continue to gain weight. Blunting that response to diet is desirable and unique to RP105/MD-1.

The RP105/MD-1 complex is not expressed in $CD45^-$ nonleukocytes in eWAT and RP105 expression is largely

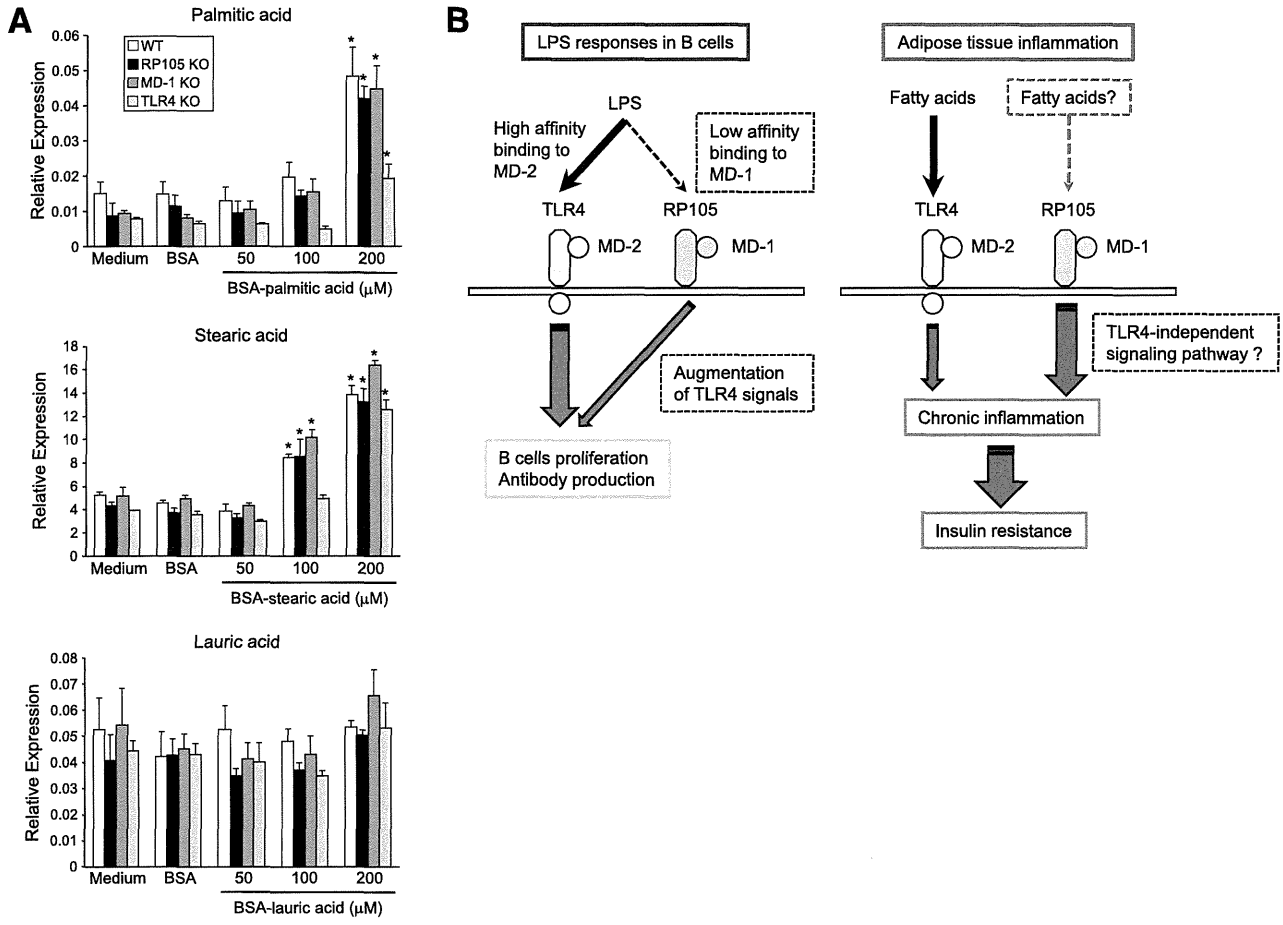

FIG. 8. Palmitate activates TLR4 but not RP105/MD-1 signaling. *A*: FAs (palmitic, stearic, and lauric acids) need to be conjugated to FA-free BSA to increase solubility. BMMs from WT, RP105 KO, MD-1 KO, and TLR4 KO mice were stimulated with the FAs conjugate to BSA or BSA control (BSA) for 24 h. Expression of TNF-α mRNA in the stimulated BMMs was measured by RT-qPCR (n = 3 per group). Data are shown as means ± SE. *P < 0.05 *vs.* BSA control. Similar results were obtained in three independent experiments. *B*: Hypothetical model of RP105/MD-1 activation in LPS responses in B cells and adipose tissue inflammation. The TLR4/MD-2 complex is essential for LPS recognition and responses. The RP105/MD-1 also could recognize LPS by low affinity and augment TLR4-dependent LPS responses in B cells. On the other hand, RP105/MD-1 might contribute to the development of adipose tissue inflammation and insulin resistance by palmitate-TLR4–independent manner.

restricted to the immune system (24). However, involvement of other cell types is possible. Signaling mediated by MyD88 can mediate HFD-induced leptin and insulin resistance in the central nervous system (38). Another report (39) suggests that TLR4 signaling in hematopoietic cells is important for obesity-associated insulin resistance. Although RP105 transcripts were low in the brain (data not shown), we observed that an HFD increased RP105 mRNA in the liver, brown adipose tissue, and skeletal muscle. Additional investigation will reveal if RP105/MD-1 has roles in those tissues.

To conclude, the RP105/MD-1 complex mediates much of the weight gain, insulin resistance, and sterile inflammation that result from exposure to an HFD. Future studies will clarify a precise ligand and signaling pathway of RP105/MD-1, which link this complex and adipose tissue inflammation.

ACKNOWLEDGMENTS

This study was supported by grants from Grant-in-Aid for Scientific Research from the Ministry of Education, Culture, Sports, Science, and Technology of the Japanese Government (20390141 and 22117509); Hokuriku Innovation Cluster for Health Science (to K.Ta.); the Uehara Memorial Foundation (to Y.N.); the Novartis Foundation (Japan) for the Promotion of Science (to Y.N.); and Takeda Science Foundation (to Y.N.).

No potential conflicts of interest relevant to this article were reported.

Y.W. conducted the experiments and wrote the manuscript. T.N. conducted the experiments. S.I. contributed to the knockout mice analysis. S.F., I.U., and K.To. contributed to the metabolic measurement data. K.Ts. contributed to the immunohistochemistry data. Y.I., T.W., and T.Sa. contributed to the energy expenditure data. Y.H., H.I., H.K., M.Sh., and M.Sa. contributed to the human study. T.Su. and Y.O. contributed to the coculture data. K.Ta. was involved in project planning, financing, and supervision. Y.N. conceived the study, conducted the experiments, and wrote the manuscript. S.A. and K.M. provided the knockout mice. Y.N. is the guarantor of this work and, as such, had full access to all of the data in the study and takes responsibility for the integrity of the data and the accuracy of the data analysis.

The authors sincerely thank Toyama Prefecture for supporting their laboratory. The authors also thank Drs. Paul W. Kincade, Oklahoma Medical Research Foundation, and Masao Kimoto, Saga University, for critical review of the manuscript. The authors thank Drs. Yoshikatsu Hirai, Ai Kariyone, Masashi Ikutani, and Tsutomu Yanagibashi, University of Toyama, for helpful suggestions. Ena Taniguchi, Yumi Miyahara, and Satoko Katsunuma, University of Toyama, are thanked for their technical assistance. The authors appreciate the secretarial assistance provided by Maki Sasaki and Ryoko Sugimoto, University of Toyama.

REFERENCES

1. Hotamisligil GS, Erbay E. Nutrient sensing and inflammation in metabolic diseases. Nat Rev Immunol 2008;8:923–934
2. Olefsky JM, Glass CK. Macrophages, inflammation, and insulin resistance. Annu Rev Physiol 2010;72:219–246
3. Lumeng CN, Bodzin JL, Saltiel AR. Obesity induces a phenotypic switch in adipose tissue macrophage polarization. J Clin Invest 2007;117:175–184
4. Fujisaka S, Usui I, Bukhari A, et al. Regulatory mechanisms for adipose tissue M1 and M2 macrophages in diet-induced obese mice. Diabetes 2009; 58:2574–2582
5. Kawai T, Akira S. The role of pattern-recognition receptors in innate immunity: update on Toll-like receptors. Nat Immunol 2010;11:373–384
6. Hoshino K, Takeuchi O, Kawai T, et al. Cutting edge: Toll-like receptor 4 (TLR4)-deficient mice are hyporesponsive to lipopolysaccharide: evidence for TLR4 as the Lps gene product. J Immunol 1999;162:3749–3752
7. Nagai Y, Akashi S, Nagafuku M, et al. Essential role of MD-2 in LPS responsiveness and TLR4 distribution. Nat Immunol 2002;3:667–672
8. Miyake K, Yamashita Y, Hitoshi Y, Takatsu K, Kimoto M. Murine B cell proliferation and protection from apoptosis with an antibody against a 105-kD molecule: unresponsiveness of X-linked immunodeficient B cells. J Exp Med 1994;180:1217–1224
9. Miyake K, Shimazu R, Kondo J, et al. Mouse MD-1, a molecule that is physically associated with RP105 and positively regulates its expression. J Immunol 1998;161:1348–1353
10. Ogata H, Su I, Miyake K, et al. The toll-like receptor protein RP105 regulates lipopolysaccharide signaling in B cells. J Exp Med 2000;192:23–29
11. Nagai Y, Shimazu R, Ogata H, et al. Requirement for MD-1 in cell surface expression of RP105/CD180 and B-cell responsiveness to lipopolysaccharide. Blood 2002;99:1699–1705
12. Nagai Y, Kobayashi T, Motoi Y, et al. The radioprotective 105/MD-1 complex links TLR2 and TLR4/MD-2 in antibody response to microbial membranes. J Immunol 2005;174:7043–7049
13. Kono H, Rock KL. How dying cells alert the immune system to danger. Nat Rev Immunol 2008;8:279–289
14. Chen GY, Nuñez G. Sterile inflammation: sensing and reacting to damage. Nat Rev Immunol 2010;10:826–837
15. Suganami T, Nishida J, Ogawa Y. A paracrine loop between adipocytes and macrophages aggravates inflammatory changes: role of free fatty acids and tumor necrosis factor alpha. Arterioscler Thromb Vasc Biol 2005;25:2062–2068
16. Shi H, Kokoeva MV, Inouye K, Tzameli I, Yin H, Flier JS. TLR4 links innate immunity and fatty acid-induced insulin resistance. J Clin Invest 2006;116: 3015–3025
17. Suganami T, Tanimoto-Koyama K, Nishida J, et al. Role of the Toll-like receptor 4/NF-kappaB pathway in saturated fatty acid-induced inflammatory changes in the interaction between adipocytes and macrophages. Arterioscler Thromb Vasc Biol 2007;27:84–91
18. Vandanmagsar B, Youm YH, Ravussin A, et al. The NLRP3 inflammasome instigates obesity-induced inflammation and insulin resistance. Nat Med 2011;17:179–188
19. Wen H, Gris D, Lei Y, et al. Fatty acid-induced NLRP3-ASC inflammasome activation interferes with insulin signaling. Nat Immunol 2011;12:408–415
20. Nakamura T, Furuhashi M, Li P, et al. Double-stranded RNA-dependent protein kinase links pathogen sensing with stress and metabolic homeostasis. Cell 2010;140:338–348
21. Oh DY, Talukdar S, Bae EJ, et al. GPR120 is an omega-3 fatty acid receptor mediating potent anti-inflammatory and insulin-sensitizing effects. Cell 2010;142:687–698
22. Rubin CS, Hirsch A, Fung C, Rosen OM. Development of hormone receptors and hormonal responsiveness in vitro: insulin receptors and insulin sensitivity in the preadipocyte and adipocyte forms of 3T3-L1 cells. J Biol Chem 1978;253:7570–7578
23. Ichioka M, Suganami T, Tsuda N, et al. Increased expression of macrophage-inducible C-type lectin in adipose tissue of obese mice and humans. Diabetes 2011;60:819–826
24. Miyake K, Yamashita Y, Ogata M, Sudo T, Kimoto M. RP105, a novel B cell surface molecule implicated in B cell activation, is a member of the leucine-rich repeat protein family. J Immunol 1995;154:3333–3340
25. Nishimura S, Manabe I, Nagasaki M, et al. CD8+ effector T cells contribute to macrophage recruitment and adipose tissue inflammation in obesity. Nat Med 2009;15:914–920
26. Hirosumi J, Tuncman G, Chang L, et al. A central role for JNK in obesity and insulin resistance. Nature 2002;420:333–336
27. Solinas G, Vilcu C, Neels JG, et al. JNK1 in hematopoietically derived cells contributes to diet-induced inflammation and insulin resistance without affecting obesity. Cell Metab 2007;6:386–397
28. Chiang SH, Bazuine M, Lumeng CN, et al. The protein kinase IKKepsilon regulates energy balance in obese mice. Cell 2009;138:961–975
29. Boden G. Interaction between free fatty acids and glucose metabolism. Curr Opin Clin Nutr Metab Care 2002;5:545–549
30. Lee JY, Sohn KH, Rhee SH, Hwang D. Saturated fatty acids, but not unsaturated fatty acids, induce the expression of cyclooxygenase-2 mediated through Toll-like receptor 4. J Biol Chem 2001;276:16683–16689
31. Inohara N, Nuñez G. ML: a conserved domain involved in innate immunity and lipid metabolism. Trends Biochem Sci 2002;27:219–221
32. Harada H, Ohto U, Satow Y. Crystal structure of mouse MD-1 with endogenous phospholipid bound in its cavity. J Mol Biol 2010;400:838–846
33. Yoon SI, Hong M, Han GW, Wilson IA. Crystal structure of soluble MD-1 and its interaction with lipid IVa. Proc Natl Acad Sci USA 2010;107:10990–10995
34. Yazawa N, Fujimoto M, Sato S, et al. CD19 regulates innate immunity by the toll-like receptor RP105 signaling in B lymphocytes. Blood 2003;102:1374–1380
35. Kanda H, Tateya S, Tamori Y, et al. MCP-1 contributes to macrophage infiltration into adipose tissue, insulin resistance, and hepatic steatosis in obesity. J Clin Invest 2006;116:1494–1505
36. Lesniewski LA, Hosch SE, Neels JG, et al. Bone marrow-specific Cap gene deletion protects against high-fat diet-induced insulin resistance. Nat Med 2007;13:455–462
37. Weisberg SP, Hunter D, Huber R, et al. CCR2 modulates inflammatory and metabolic effects of high-fat feeding. J Clin Invest 2006;116:115–124
38. Kleinridders A, Schenten D, Könner AC, et al. MyD88 signaling in the CNS is required for development of fatty acid-induced leptin resistance and diet-induced obesity. Cell Metab 2009;10:249–259
39. Saberi M, Woods NB, de Luca C, et al. Hematopoietic cell-specific deletion of toll-like receptor 4 ameliorates hepatic and adipose tissue insulin resistance in high-fat-fed mice. Cell Metab 2009;10:419–429

Hepatology Research

Hepatology Research 2012; 42: 543–548 doi: 10.1111/j.1872-034X.2012.00978.x

Review Article

Interplay between bone marrow and liver in the pathogenesis of hepatic fibrosis

Yutaka Inagaki and Reiichi Higashiyama*

Department of Regenerative Medicine, Tokai University School of Medicine and the Institute of Medical Sciences, Isehara, Japan

Recent advances in the technologies of both molecular biology and regenerative medicine have made it possible to identify bone marrow (BM)-derived cells migrating into various fibrotic organs including the liver. A number of studies have reported that BM-derived cells migrating into fibrotic liver tissue exhibit a myofibroblast-like phenotype and may participate in the progression of liver fibrosis. On the other hand, it has also been shown that BM-derived cells express matrix metalloproteinases and contribute to the regression of experimental liver fibrosis. These contradictory results may arise, at least in part, from the uncertainty of various different methods that have been used in those studies. In this review article, we describe the interplay between BM and liver in the progression and regression of liver fibrosis, with an emphasis on the necessity of qualified methods with high specificity and sensitivity to evaluate the role of BM-derived cells in collagen production.

Key words: bone marrow, collagen, liver fibrosis, matrix metalloproteinase, regenerative medicine

INTRODUCTION

IRRESPECTIVE OF THE etiologies of hepatic injury, liver fibrosis is caused commonly by a chronic and uncontrolled inflammatory/repair process leading to excessive deposition of collagen and other components of extracellular matrix. Collagen contents in tissue are under control of a dynamic balance between its production and degradation by matrix metalloproteinases (MMPs), and a disruption of this equilibrium results in tissue fibrosis in various organs including the liver. Hepatic stellate cells (HSC) are the main producers of collagen in fibrotic liver,[1] but they also express MMP-13,[2] the major interstitial collagenase that degrades collagen in rodents.

Correspondence: Professor Yutaka Inagaki, Department of Regenerative Medicine, Tokai University School of Medicine, 143 Shimo-kasuya, Isehara, Kanagawa 259-1193, Japan. Email: yutakai@is.icc.u-tokai.ac.jp

**Present address*: Southern California Research Center for ALPD and Cirrhosis, Keck School of Medicine of the University of Southern California, Los Angeles, CA, USA

Received 20 August 2011; revision 1 January 2012; accepted 22 January 2012.

Recent advances in the technologies of both molecular biology and regenerative medicine have made it possible to identify bone marrow (BM)-derived cells migrating into fibrotic organs such as liver, lung and skin.[3] Consequently, a number of studies have reported that BM-derived cells migrating into fibrotic liver tissue exhibit a myofibroblast-like phenotype and may participate in the progression of liver fibrosis. On the other hand, we have shown that BM-derived stem/progenitor cells express MMP-13 and MMP-9, and contribute to the spontaneous regression of experimental liver fibrosis after the cessation of repeated carbon tetrachloride (CCl_4) injections.[4]

These contradictory results may arise, at least in part, from the uncertainty of various different methods that have been used in those studies. In this review article, we summarize the current concept of interplay between BM and liver in the progression and regression of liver fibrosis from the viewpoint of production of collagen and MMP by BM-derived cells. We would like to discuss the technical limitations of the methods that are currently used for identification of BM origin and demonstration of collagen expression, and emphasize the necessity of qualified methods with high specificity and sensitivity

to evaluate the role of BM in the pathogenesis of liver fibrosis.

REGRESSION OF LIVER FIBROSIS BY BM-DERIVED CELLS

OUR PREVIOUS STUDY has shown that BM-derived stem/progenitor cells express MMP-13 and MMP-9, and contribute to the spontaneous regression of experimental liver fibrosis after the cessation of repeated CCl_4 injections.[4] In order to determine the BM origin of cells, BM of wild type mice was replaced with cells from transgenic animals that ubiquitously express enhanced green fluorescent protein (EGFP) before starting CCl_4 injections. Administration of granulocyte-colony stimulating factor (G-CSF) and overexpression of hepatocyte growth factor (HGF) synergistically enhanced MMP-9 expression in fibrotic liver and accelerated the resolution of liver fibrosis.[4] Interestingly, some of the EGFP-positive BM-derived cells co-expressed stromal cell-derived factor-1 (SDF-1), indicating that they themselves may enhance the mobilization of cells from BM (Fig. 1).

A subsequent study by others further supported the contribution of BM cells to the resolution of liver fibrosis.[5] In this study, the authors performed myeloablation and BM reconstitution during the ongoing liver fibrosis induced by repeated CCl_4 injections. An HGF gene transfer into skeletal muscles of the recipient mice stimulated the expression of SDF-1, accelerated the recruitment of BM-derived cells into fibrotic liver, and enhanced gelatinase activities.[5] Moreover, several studies of therapeutic infusions of BM cells have indicated that BM-derived cells express MMPs and contribute to the regression of experimental liver fibrosis.[6,7] Based on the results of these experimental studies, there have been an increasing number of clinical trials of autologous BM cell infusion therapy to treat patients with critical liver diseases including advanced liver cirrhosis.[8–12]

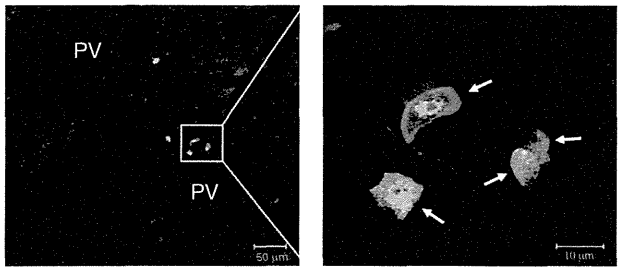

Figure 1 Stromal cell-derived factor-1 (SDF-1) expression in bone marrow (BM)-derived cells migrating into fibrotic liver. Transgenic mice that ubiquitously express enhanced green fluorescent protein by the cytomegalovirus enhancer and the chicken β-actin promoter (CAG/EGFP) were used as a BM donor. Liver specimens from CCl_4-treated CAG/EGFP recipient mice were stained with specific antibodies recognizing SDF-1. Nuclei were stained with propidium iodide. A part of the left panel is shown in higher magnification in the right panel. EGFP-positive BM-derived cells that co-express SDF-1 are indicated by *arrows*. *PV*, portal vein. *Scale bars*, 50 μm (left panels) or 10 μm (right panels).

POSSIBLE PARTICIPATION OF BM-DERIVED CELLS IN HEPATIC FIBROGENESIS

ON THE OTHER hand, there have been a number of experimental and human studies showing differentiation of BM cells into potential collagen-producing cells such as HSC,[13,14] myofibroblasts[15,16] and fibrocytes,[17] thus their possible participation in the progression of liver fibrosis. These findings are in agreement with the results of a number of studies showing functional contribution of blood-borne collagen-producing cells to tissue repair or fibrosis in various other organs.[3,18,19] The presence of mesenchymal stem cells (MSC) in BM, which have a potential to differentiate into not only hepatocytes but also mesenchymal cell lineages such as osteoblasts, chondrocyte and adipocytes, raises a concern that these cells participate in the progression of fibrosis by producing collagen in the liver.[20]

TECHNICAL LIMITATIONS TO IDENTIFY BM ORIGIN AND DEMONSTRATE COLLAGEN EXPRESSION

A SERIES OF studies described above have given a serious caution that BM-derived cells possess profibrotic phenotypes.[21] However, these previous studies used different methods, the fluorescent *in situ* hybridization to detect Y chromosomes (Y-FISH) or genetic EGFP labeling of BM cells, to identify BM origin. They demonstrated the collagen-producing cells by either direct immunohistochemical staining of collagen or demonstration of fibrogenic cell markers such as α-smooth muscle actin (αSMA). Thus, direct contribution of BM-derived cells to collagen production during hepatic fibrogenesis has not been fully verified for the following critical reasons.[22]

Limitation using Y-FISH

Some of the previous studies used Y-FISH in sex-mismatched BM transplantation experiments.[15,16] These

studies showed the expression of αSMA in the Y-FISH-proven male transplanted cells migrating into female fibrotic liver tissue. However, it is impossible to demonstrate the exact co-localization of fluorescent Y chromosome signal (nucleus) and αSMA expression (cytoplasm) in individual cells unless using the 3-dimensional and rotational analyses of confocal microscopic images.[22]

Presence of autofluorescence in fibrotic liver tissue

Meanwhile, others used EGFP as a genetic marker of BM cells.[13,14,17] However, while immunohistochemical detection of EGFP has a limitation in the specificity of immunostaining, direct observation of EGFP fluorescence is often hampered by the presence of autofluorescence in fibrotic liver tissue, leading to misinterpretation of obtained results even using a confocal microscope.[4]

Difficulty to prove cellular source of collagen in fibrotic tissue

It is also difficult to demonstrate collagen production by BM-derived cells present within the fibrous tissue. Because of an abundant amount of extracellular collagen accumulated around the cells, it is not easy to determine precisely whether these cells certainly produce collagen, or they are merely surrounded by collagen fibers. Therefore, most of the previous studies[13,15,16,20] failed to demonstrate clear collagen production by BM-derived cells, and relied primarily on the morphology of "myofibroblast-like cells" present in the fibrous tissue and/or their expression of αSMA and other markers of activated HSC.

Heterogeneity of αSMA expression in collagen-producing cells

Finally, even if some of the cells exhibit the feature of αSMA-positive myofibroblasts, it does not necessarily mean that they produce collagen and contribute directly to the progression of liver fibrosis.[23] It is now well recognized that αSMA-positive activated HSC is not the only source of collagen in fibrotic liver, but different types of cells such as portal fibroblasts express collagen and participate in the progression of liver fibrosis depending on the etiologies of liver injury and fibrosis.[24] Thus, the cellular entity of BM-derived collagen-producing cells, if present, has not been established yet.

ESTABLISHMENT OF A SPECIFIC AND SENSITIVE METHOD TO EVALUATE COLLAGEN PRODUCTION

CONSIDERING THE LIMITATIONS in the previous studies described above, we tried to evaluate the direct contribution of BM-derived cells to collagen production by using more specific and quantitative methods.[22,25] For this purpose, we established a transgenic mouse strain that harbors the tissue-specific enhancer and promoter sequences of α2 type I collagen gene (*Col1a2*) linked to either an *EGFP* (COL/EGFP) or *luciferase* (COL/LUC) reporter gene. The −17 000 to −15 500 *Col1a2* sequence has a strong enhancer activity that directs tissue-specific gene expression only in collagen-producing cells such as osteoblasts and skin fibroblasts during embryonic development.[26,27] Furthermore, we have previously shown that *Col1a2* promoter is activated with this enhancer following CCl_4 injections.[28]

These transgenic reporter mice were used for BM transplantation experiments as schematically shown in Figure 2. EGFP expression can be observed in type I collagen-producing cells independently of their origins in transgenic COL/EGFP mice. On the other hand, when BM of wild type mice is replaced with cells from COL/EGFP mice, EGFP-expressing cells in the fibrotic liver, if present, represent exclusively BM-derived collagen-producing cells. Similarly, by comparing the luciferase

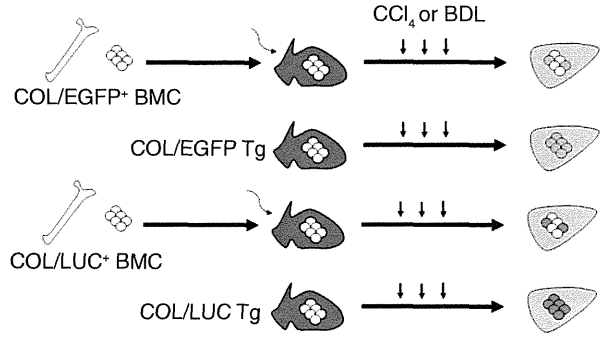

Figure 2 A specific and sensitive experimental system to evaluate the role of bone marrow (BM) in collagen production. Whole bone marrow cells (*BMC*) obtained from transgenic COL/EGFP or COL/LUC mice were injected into the irradiated C57BL/6 wild type animals. Those recipient mice underwent either repeated carbon tetrachloride injections (CCl_4) or ligation of the common bile duct (*BDL*). Transgenic COL/EGFP and COL/LUC mice (*Tg*) were also included as controls. Modified from the article by Higashiyama *et al.* (2009).[22] COL/EGFP, *Col1a2* linked to an EGFP reporter gene; COL/LUC, *Col1a2* linked to luciferase reporter gene.

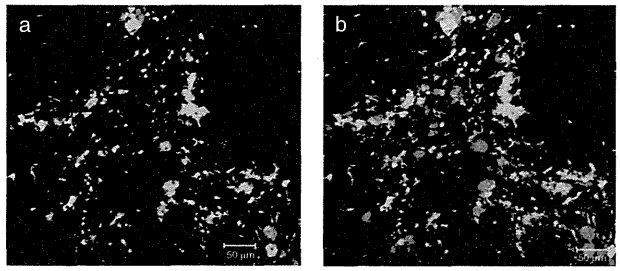

Figure 3 Identification of specific fluorescent signals in fibrotic liver tissue. By using the emission fingerprinting method, a mixture of specific and non-specific fluorescent signals in panel a can be separated into the specific enhanced green fluorescent protein (EGFP) fluorescence and non-specific autofluorescence in panel b. Representative pictures are shown of fibrotic liver tissue obtained from transgenic COL/EGFP mice following repeated CCl_4 injections. *Scale bars*, 50 μm. Modified from the article by Higashiyama *et al.* (2007).[4]

activities in liver tissue between transgenic COL/LUC mice and their BM recipients, estimate can be made quantitatively of the relative contribution of liver resident and BM-derived cells to collagen production during hepatic fibrogenesis.

Moreover, in order to eliminate the background autofluorescence and identify only the specific EGFP fluorescence, we used the emission fingerprinting method[29] that successfully eliminated the background auto-fluorescence (Fig. 3).[4,22]

LITTLE CONTRIBUTION OF BM-DERIVED CELLS TO COLLAGEN PRODUCTION DURING HEPATIC FIBROGENESIS

WITH SUCH CAREFUL consideration on the specificity of the results, we have clearly demonstrated a lack of *Col1A2* promoter activation in BM-derived cells following the two different fibrogenic stimuli, repeated CCl_4 injections and the ligation of the common bile duct.[22] The same results were obtained in both the initial and advanced stages of liver fibrosis, after 4 weeks of CCl_4 injections and a 3 month-length of chronic CCl_4 intoxication, respectively.[22] However, considering the long time duration needed for the development of liver cirrhosis in humans, it is still possible that BM-derived cells may participate differentially in collagen production depending on the stages of liver fibrosis.

Moreover, when the same experimental system was applied for murine dermal fibrosis, a limited but significant number of EGFP-positive BM-derived collagen-producing cells were observed following repeated subcutaneous bleomycin injections into COL/EGFP recipient mice, and such collagen-producing cells derived from BM represented approximately 5% of total collagen-producing cells.[25] Similarly, a previous study using the same transgenic COL/LUC mice and their BM recipients showed that the luciferase activity was dramatically increased in the scar area of the heart following experimental myocardial infarction.[19] In contrast, another experiment using COL/LUC mice failed to demonstrate the contribution of BM-derived cells to collagen production in renal fibrosis induced by unilateral ureteric obstruction.[30] Collectively, it could be argued that the extent of contribution of BM-derived cells to collagen production during the progression of organ fibrosis may vary depending on the etiologies and/or duration of tissue injury, the sites of affected organs, and the stages of tissue fibrosis.

A previous study using another kind of EGFP reporter mice driven by the enhancer and promoter regions of the coordinately expressed α1 type I collagen gene (*Col1a1*) implicated fibrocytes in collagen production in the progression of liver fibrosis.[17] Apart from that they used immunohistochemical staining of EGFP rather than detecting EGFP fluorescence, the reasons for the discrepancies between their results and ours are unknown. However, a subsequent study using the same *Col1a1/EGFP* reporter mice denied the direct roles of fibrocytes in collagen production during renal or dermal fibrosis.[31]

FUTURE PERSPECTIVES

AS BM CONSISTS of a variety of cells with different properties and functions, there are many aspects of pathophysiological correlations observed between BM and the liver. In this brief review article on liver fibrosis, we have focused only on the direct roles of BM-derived cells in collagen and MMP expression. However, cells from BM apparently participate in liver fibrogenesis through other mechanisms such as production of inflammatory cytokines and growth factors. Along the same line, fibrocytes are reported to be potent antigen-presenting cells capable of priming naïve T cells.[32]

The heterogeneity of BM cells raises a critical question as to what kinds of cells are most efficient to resolve liver fibrosis.[33] A previous study implicated a subpopulation of Liv-8-negative non-hematopoietic BM cells,[6] leading to the clinical application of MSC therapy for patients with liver failure caused by hepatitis B virus infection.[34] Others reported the usefulness of endothelial progenitor cells to treat experimental liver fibrosis.[7] A more recent

study has shown that a therapeutic infusion of BM-derived macrophage improves murine fibrosis by increasing MMP-13 and MMP-9 expression by endogenous effector cells, whereas that of unfractionated BM cells even worsens it.[35] Clarification of this point will certainly contribute to the development of more effective cell therapy for liver fibrosis in the clinical setting.[33]

It should be noted, however, that the behaviors and fates are not always the same between mobilized endogenous BM cells and infused exogenous cells. The committed cells mobilized from BM may express certain cell surface ligands/receptors and secrete several humoral factors in fibrotic liver tissue, which may not be the case in artificially infused cells. In addition, isolation and infusion of autologous BM cells are invasive procedures that need general anesthesia. Thus, if the therapeutic recruitment of autologous BM cells and their differentiation into MMP-expressing cells can be effectively achieved, it will be obviously a safer and less invasive approach for the treatment of liver fibrosis.[36] To this end, work is necessary to elucidate not only the humoral factors but also the nature of microenvironmental niche in fibrotic liver tissue that regulate the homing and differentiation of BM-derived cells.

ACKNOWLEDGMENTS

OUR STUDY PRESENTED in this review article was supported in part by a grant-in-aid from the Ministry of Education, Culture, Sports, Science and Technology, Japan, and by research grants from Mitsukoshi Health and Welfare Foundation, Mitsui Life Social Welfare Foundation, the Cosmetology Research Foundation, Kanagawa Nanbyo Study Foundation, and the Smoking Research Foundation. We are indebted to Professor Isao Okazaki, International University of Health and Welfare, for his continuous support and encouragement throughout the work.

REFERENCES

1 Friedman SL. Cellular sources of collagen and regulation of collagen production in liver. *Semin Liver Dis* 1990; **10**: 20–9.
2 Watanabe T, Niioka M, Hozawa S *et al.* Gene expression of interstitial collagenase in both progressive and recovery phase of rat liver fibrosis induced by carbon tetrachloride. *J Hepatol* 2000; **33**: 224–35.
3 Direkze NC, Forbes SJ, Brittan FM *et al.* Multiple organ engraftment by bone-marrow-derived myofibroblasts and fibroblasts in bone-marrow-transplanted mice. *Stem Cells* 2003; **21**: 514–20.
4 Higashiyama R, Inagaki Y, Hong YY *et al.* Bone marrow-derived cells express matrix metalloproteinases and contribute to regression of liver fibrosis in mice. *Hepatology* 2007; **45**: 213–22.
5 Asano Y, Iimuro Y, Son G *et al.* Hepatocyte growth factor promotes remodeling of murine liver fibrosis, accelerating recruitment of bone marrow-derived cells into the liver. *Hepatol Res* 2007; **37**: 1080–94.
6 Sakaida I, Terai S, Yamamoto N *et al.* Transplantation of bone marrow cells reduces CCl_4-induced liver fibrosis in mice. *Hepatology* 2004; **40**: 1304–11.
7 Nakamura T, Torimura T, Sakamoto M *et al.* Significance and therapeutic potential of endothelial progenitor cell transplantation in a cirrhotic liver rat model. *Gastroenterology* 2007; **133**: 91–107.
8 am Esch IIJS, Knoefel WT, Klein M *et al.* Portal application of autologous $CD133^+$ bone marrow cells to the liver: a novel concept to support hepatic regeneration. *Stem Cells* 2005; **23**: 463–70.
9 Gordon MY, Levicar N, Pai M *et al.* Characterization and clinical application of human $CD34^+$ stem/progenitor cell populations mobilized into the blood by granulocyte colony-stimulating factor. *Stem Cells* 2006; **24**: 1822–30.
10 Terai S, Ishikawa T, Omori K *et al.* Improved liver function in patients with liver cirrhosis after autologous bone marrow cell infusion therapy. *Stem Cells* 2006; **24**: 2292–8.
11 Gasbarrini A, Rapaccini GL, Rutella S *et al.* Rescue therapy by portal infusion of autologous stem cells in a case of drug-induced hepatitis. *Dig Liver Dis* 2007; **39**: 878–82.
12 Lyra AC, Soares MB, da Silva LF *et al.* Feasibility and safety of autologous bone marrow mononuclear cell transplantation in patients with advanced chronic liver diseases. *World J Gastroenterol* 2007; **13**: 1067–73.
13 Baba S, Fujii H, Hirose T *et al.* Commitment of bone marrow cells to hepatic stellate cells in mouse. *J Hepatol* 2004; **40**: 255–60.
14 Miyata E, Masuya M, Yoshida S *et al.* Hematopoietic origin of hepatic stellate cells in the adult liver. *Blood* 2008; **111**: 2427–35.
15 Forbes SJ, Russo FP, Rey V *et al.* A significant proportion of myofibroblasts are of bone marrow origin in human liver fibrosis. *Gastroenterology* 2004; **126**: 955–63.
16 Russo FP, Alison MR, Bigger BW *et al.* The bone marrow functionally contributes to liver fibrosis. *Gastroenterology* 2006; **130**: 1807–21.
17 Kisseleva T, Uchinami H, Feirt N *et al.* Bone marrow-derived fibrocytes participate in pathogenesis of liver fibrosis. *J Hepatol* 2006; **45**: 429–38.
18 Hashimoto N, Jin H, Liu T *et al.* Bone marrow-derived progenitor cells in pulmonary fibrosis. *J Clin Invest* 2004; **113**: 243–52.
19 van Amerongen MJ, Bou-Gharios G, Popa ER *et al.* Bone marrow-derived myofibroblasts contribute functionally to scar formation after myocardial infarction. *J Pathol* 2008; **214**: 377–86.

20 di Bonzo LV, Ferrero I, Cravanzola C *et al.* Human mesenchymal stem cells as a two-edged sword in hepatic regenerative medicine: engraftment and hepatocyte differentiation versus profibrogenic potential. *Gut* 2008; **57**: 223–31.
21 Kallis YN, Alison MR, Forbes SJ. Bone marrow stem cells and liver disease. *Gut* 2007; **56**: 716–24.
22 Higashiyama R, Moro T, Nakao S *et al.* Negligible contribution of bone marrow-derived cells to collagen production during hepatic fibrogenesis in mice. *Gastroenterology* 2009; **137**: 1459–66.
23 Magness ST, Bataller R, Yang L *et al.* A dual reporter gene transgenic mouse demonstrates heterogeneity in hepatic fibrogenic cell populations. *Hepatology* 2004; **40**: 1151–9.
24 Beaussier M, Wendum D, Schiffer E *et al.* Prominent contribution of portal mesenchymal cells to liver fibrosis in ischemic and obstructive cholestatic injuries. *Lab Invest* 2007; **87**: 292–303.
25 Higashiyama R, Nakao S, Shibusawa Y *et al.* Differential contribution of dermal resident and bone marrow-derived cells to collagen production during wound healing and fibrogenesis in mice. *J Invest Dermatol* 2011; **131**: 529–36.
26 Bou-Gharios G, Garrett LA, Rossert J *et al.* A potent far-upstream enhancer in the mouse proα2(I) collagen gene regulates expression of reporter genes in transgenic mice. *J Cell Biol* 1996; **134**: 1333–44.
27 De Val S, Ponticos M, Antoniv TT *et al.* Identification of the key regions within the mouse pro-α2(I) collagen gene far-upstream enhancer. *J Biol Chem* 2002; **277**: 9286–92.
28 Inagaki Y, Truter S, Bou-Gharios G *et al.* Activation of proα2(I) collagen promoter during hepatic fibrogenesis in transgenic mice. *Biochem Biophys Res Commun* 1998; **250**: 606–11.
29 Usuku T, Nishi M, Morimoto M *et al.* Visualization of glucocorticoid receptor in the brain of green fluorescent protein-glucocorticoid receptor knock in mice. *Neuroscience* 2005; **135**: 1119–28.
30 Roufosse C, Bou-Gharios G, Prodromidi E *et al.* Bone marrow-derived cells do not contribute significantly to collagen I synthesis in a murine model of renal fibrosis. *J Am Soc Nephrol* 2006; **17**: 775–82.
31 Lin S-L, Kisseleva T, Brenner DA *et al.* Pericytes and perivascular fibroblasts are the primary source of collagen-producing cells in obstructive fibrosis of the kidney. *Am J Pathol* 2008; **173**: 1617–27.
32 Chesney J, Bacher M, Bender A *et al.* The peripheral blood fibrocyte is a potent antigen-presenting cell capable of priming naïve T cells *in situ*. *Proc Natl Acad Sci USA* 1997; **94**: 6307–12.
33 Stutchfield BM, Forbes SJ, Wigmore SJ. Prospects for stem cell transplantation in the treatment of hepatic disease. *Liver Transpl* 2010; **16**: 827–36.
34 Peng L, Xie D-Y, Lin B-L *et al.* Autologous bone marrow mesenchymal stem cell transplantation in liver failure patients caused by hepatitis B: short-term and long-term outcomes. *Hepatology* 2011; **54**: 820–8.
35 Thomas JA, Pope C, Wojtacha D *et al.* Macrophage therapy for murine liver fibrosis recruits host effector cells improving fibrosis, regeneration, and function. *Hepatology* 2011; **53**: 2003–15.
36 Inagaki Y, Higashiyama R, Okazaki I. Treatment strategy for liver fibrosis through recruitment and differentiation of bone marrow stem/progenitor cells. *Hepatol Res* 2007; **37**: 991–3.

Novel Strategies for Hepatocellular Carcinoma Based on MMPs Science

Isao Okazaki[1,*] and Yutaka Inagaki[2]

[1]*Department of Internal Medicine, Sanno Hospital and University Hospital, International University of Health and Welfare, Tokyo and Tochigi Prefecture, Japan;* [2]*Department of Regenerative Medicine, Tokai University School of Medicine, Isehara, Kanagawa Prefecture, Japan*

Abstract: Hepatocellular carcinoma (HCC) is a cancer with extremely poor prognosis. This review discusses the pathological characteristics of multi-step hepatocarcinogenesis, tumor growth, invasion and metastasis, the expression of matrix metalloproteinases (MMPs) and their inhibitors *via* signal transduction in relation to dedifferentiation of hepatoma cells. It introduces the reports on anti-cancer agents in the field of MMP science, and finally describes novel strategies for the early stages of HCC in relation to cancer stem cells.

Keywords: Hepatocellular carcinoma (HCC), Hepatitis B virus (HBV), Hepatitis C virus (HCV), Alcoholic liver diseases, Non-alcoholic liver diseases, Bone marrow-derived stem cell, Matrix metalloproteinase (MMP), Tissue inhibitor of metalloproteinase (TIMP), Cancer invasion, Cancer metastasis, Cancer treatment, Anti-cancer agents.

1. INTRODUCTION

Hepatocellular carcinoma (HCC) is the third leading cause of cancer-related mortality in the world, responsible for more than 600,000 deaths annually [1]. Epidemiological studies have revealed that 50% to 80% of HCC cases are related to hepatitis B virus (HBV) infection, and 10% to 25% are thought to be the result of hepatitis C virus (HCV) infection [2]. Geographical endemic infection in the world varies; in China nearly 99% HCC are reported to be HBV-related while 12% is HCV-related in another report; in Gambia HBV-related HCC 61% while HCV-related HCC 19%; in Japan HBV-related HCC is 15% and HCV-related HCC 61%; in the USA HBV-related HCC is 16% and HCV-related 36% [2]. HCC patients with HBV (with HIV) or HCV have shown HBV- or HCV-related chronic hepatitis and/or liver cirrhosis prior to development of HCC [2, 3]. In the USA 22% of HCC cases is associated with alcohol-induced liver disease and more than 40% of HCC are associated with diabetes, non-alcoholic fatty liver disease (NAFLD) and non-alcoholic steatohepatitis (NASH) [2]. Diabetes and obesity are implicated in NAFLD and NASH. In developed countries (Japan, USA, Europe) HCV-related HCC decrease, but a new trend in HCC development is rising with changes in the environment and lifestyles with the growing burden of diabetes and obesity [2].

Recent diagnostic techniques for detecting early HCC and treatment choices including surgery and chemotherapeutic agents for advanced HCC have made remarkable progress in the developed countries, but the prognosis for HCC remains unsatisfactory [3,4]. The factors determining the prognosis of HCC depend on the ability of hepatoma cells to invade the fibrous capsule surrounding the tumor nodules as well as portal triads, and to cause intra-hepatic and/or extra-hepatic (especially lung, bone, adrenal gland, and other) metastasis [3-5].

The authors have investigated the mechanism of liver fibrosis from the viewpoint of collagen formation and degradation [6-21] as well as the mechanism of the invasion and metastasis of cancer cells [22-24]. Here, the authors review recent reports on *in situ* hybridization to detect mRNAs of both MMPs including ADAMs/ADAMTSs and TIMPs and immunohistochemical localization of their proteins related to cancer invasion with/without metastasis, introduce anti-cancer agents reported from the viewpoints of MMPs and TIMPs, and finally describe novel strategies for the early stages of HCCas related to cancer stem cells.

*Address correspondence to this author at the Department of Internal Medicine, Sanno Hospital, International University of Health and Welfare, 8-10-16 Akasaka, Minato-ku, Tokyo 107-0052, Japan; Tel: +81-3-3402-3151; Fax: +81-3-3404-3652; E-mail: iokazaki@iuhw.ac.jp

2. PATHOLOGICAL CHARACTERISTICS OF HCC

Advanced HCC shows a large tumor mass composed of several small nodules (called "nodules in nodule") surrounded by thick fibrous bands. Hepatoma cells show different differentiation stages from one nodule to another, but exhibit the same differentiation stages in each single nodule [3, 5, 25].

A nodule of early HCC smaller than 2 cm in diameter is composed of well-differentiated and moderately differentiated cancer cells, as shown in Fig. (**1**) [25]. Portal tracts and fibrotic septa of cirrhosis remain within the nodule of early HCC. These structures disappear gradually as the nodule grows in size. This disappearance seems to be correlated with stromal invasion by well-differentiated cancer cells [26]. Well-differentiated cancer cells are thought to destroy fibrous tissue such as portal tracts and fibrous bands in cirrhotic liver [26].

A multi-step hepatocarcinogenesis and subsequent progression have been clarified [27-29]. That is, the formation of atypical lesions increases in order from adenomatous hyperplasia to atypical adenomatous hyperplasia, then to early HCC composed of well-differentiated cancer cells. As the tumor increases in size, foci of less differentiated malignant tissues arise in the well-differentiated tumor and increase until they replace the well differentiated tumor tissues [29]. Moderately differentiated cancer cells appear within the group of well-differentiated cancer cells, compress them outward, and a fibrotic capsule between well and moderately differentiated cancer cells is formed, resulting in a fibrous capsule surrounding advanced HCC. Thus, advanced HCC with nodules in nodule with thick fibrous bands is formed [3, 25-29].

Several histopathological features of liver cancers are described in the textbook by Okuda and Takasu [3]. The present review focuses on HCC excluding cholangiocarcinoma, hepatoblastoma, epithelial hemangioendothelioma, angiosarcoma, undifferentiated embryonal sarcoma, and malignant sarcoma.

3. LOCALIZATION OF MMPs AND TIMPs IN HCC

Cancer cells of HCC are characterized by their invasion to the portal tracts and the thick fibrous bands of liver cirrhosis as noted above. The enzymes responsible for the degradation of the

1875-5992/12 $58.00+.00

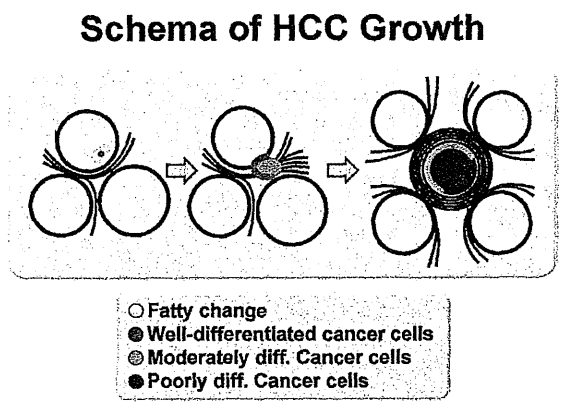

Fig. (1). Multi-step hepatocarcinogenesis. Well-differentiated hepatoma cells (red) arise within the nodules of hepatocytes with fatty metamorphosis (yellow) in liver cirrhosis. Less diferentiated, moderately differentiated, hepatoma cells (green) arise within the nest of well-differentiated hepatoma cells. Moderately differentiated cells proliferate rapidly, compress and replace well-differentiated hepatoma cells. Finally, well-differentiated hepatoma cells disappear, and poorly differentiated hepatoma cells (dark brown) arise and occupy against moderately differentiated hepatoma cells.

extracellular matrix (ECM) including basement membrane have been shown to be associated with MMPs and TIMPs, especially MMP-2 and MMP-9 [30, 31]. The correlation of the clinical and pathological characteristics of invasion/metastasis and the expression of MMPs and TIMPs in both mRNA and protein levels have been reported (Table **1**) [22, 33-51].

Cells responsible for the production of MMPs and TIMPs, their specific mRNA and protein, have been observed. The results, however, are not the same in the 21 papers listed in Table **1**. The factors responsible for the differences in observations are thought to be due to the stage of HCC patients reported, variable extents of tumor dedifferentiation, grade of the concomitant liver fibrosis seen in the high incidence of HCC, causes of HCC, treatment with/without chemotherapy, arterial embolization, previous surgical resection, etc. Moreover, the differences in the methods used in the reports needed to be considered.

The histological distribution and intensity of mRNAs and proteins of MMPs and TIMPs in normal liver and liver fibrosis are described briefly below, followed by discussion of those in human HCC cases.

3.1. MMPs and TIMPs in Human Normal Liver and Liver Fibrosis

3.1.1. MMPs in Human Normal Liver

In human normal livers, MMP-2 mRNA distribution is restricted to fibroblasts and endothelial cells within portal tracts and scattered sinusoidal cells, but not observed in bile ducts and hepatocytes by *in situ* hybridization [37]. mRNA expression of other MMPs in human normal liver have not been investigated.

3.1.2. MMPs in Human Liver Fibrosis

The authors published a review on the role of MMPs and TIMPs in the formation of experimental liver fibrosis as well as in the recovery from liver cirrhosis by *in situ* hybridization using specific cDNA [52]. However, the observed findings were based on experimental models in rats.

In human liver fibrosis MMPmRNA was not expressed in hepatocytes but was positive in stromal fibroblasts, stellate cells and some portions of bile duct epithelium and endothelial cells [37, 39]. The intensity of expression depended on the inflammatory changes such as chronic active hepatitis showing not only severe fibrosis but also inflammatory cell infiltration resulting in the destruction of portal triads [37, 39].

3.1.3. TIMPs in Normal Liver

By Northern blot hybridization TIMP-1 expression was observed, but TIMP-2 expression was very weak and even below the detectable level [35]. *In situ* hybridization revealed that transcripts for TIMP-1 were found in hepatocytes, bile duct cells, sinusoidal lining cells, endothelial cells of the vessels, and stromal cells [35]. Among these, the signal intensity of the transcript was high in sinusoidal cells and bile duct cells [35]. The distribution of TIMP-1 expression was intense in the periportal hepatocytes, while it was sparse around the terminal hepatic veins [35]. TIMP-2 expression was weak, but some sinusoidal lining cells and stromal cells were stained positively [35]. TIMP-2 mRNA distribution was restricted to fibroblasts and endothelial cells within portal tracts and scattered sinusoidal cells by *in situ* hybridization [37, 39].

3.1.4. TIMPs in Liver Fibrosis

Not only hepatocytes but also stromal fibroblast, stellate cells, sinusoidal endothelial cells and inflammatory cells in the fibrous bands also expressed TIMP-1 mRNA and TIMP-2 mRNA [37, 39].

3.2. MMPs in Advanced Stage of HCC

Since MMP-2 and MMP-9 were noted in cancer invasion and metastasis [30, 31], MMP-2 and MMP-9 in HCC were investigated earlier than the studies on MMP-1 and other MMPs.

MMP-9: The subjects of Arii *et al.* [34] were advanced HCC patients who had undergone surgical treatment. Arii *et al.* [34] observed transcripts for MMP-2 and MMP-9 in the tumorous liver samples and compared with those in the adjacent non-tumorous liver samples obtained from surgical specimens. Transcripts for MMP-9 were detected in tumorous tissues in 16 of the 23 HCC samples, and 15 of 16 positive samples showed stronger expression in the tumorous tissues than in the non-tumorous tissues. The correlation of MMP-9 expression and the presence of capsular invasion by conventional microscopical observation suggested that MMP-9 closely participated in capsular infiltration in HCC. Histological demonstration for MMP-9 protein showed strong staining in hepatoma cells, especially in the marginal area of the tumorous tissue, stromal fibroblasts, epithelial cells of the bile ducts and vascular endothelial cells [34].

Ashida *et al.* [43] reported that MMP-9 mRNA was expressed in hepatoma cells of 22 of 27 HCC samples by *in situ* hybridization. Expression of MMP-9 mRNA was seen in 86% of well-differentiated HCC, 86% of moderately differentiated HCC and 75% of poorly differentiated HCC. In this study there was no significant difference in mRNA expression of MMP-9 among the histological grades of HCC. Strong expression of MMP-9 mRNA was shown in hepatoma cells at the invasion sites of both capsules and portal veins. The distribution of MMP-9 transcripts in cancer nodules was mostly homogeneous, but the signal intensity varied with the nodules. Immunohistochemical study showed that the protein of MMP-9 was stained at the periphery of cancer nodule whereas the transcripts were distributed homogeneously in hepatoma cells within the nodule [43].

MMP-9 production (or mRNA expression) was seen in hepatoma cells [42, 44] and may be involved in stromal invasion and metastasis within nodules. Some scattered stromal fibroblasts and endothelial cells expressed MMP-9 mRNA at weak levels [43, 45].

MMP-2 and MT1-MMP: Since Sato *et al.* [53] identified MT1-MMP and the activation mechanism of pro-MMP-2 by MT1-MMP and TIMP-2 on the cell surface was reported [54], there have been several papers investigating MMP-2, TIMP-2 and/or MT1-MMP in HCC [34, 36-39, 41-51]. Most of them [38, 42, 45, 47-51] showed strong expression of mRNAs and proteins of both MT1-